Astronomy & Astrophysics manuscript no. beta˙pic˙V5
July 7, 2017

The β Pictoris association low-mass members: membership assessment, rotation period distribution, and dependence on multiplicity*

S. Messina[1], A.C. Lanzafame[2,1], L. Malo[3], S. Desidera[4], A. Buccino[5,6], L. Zhang[7], S. Artemenko[8] M. Millward[9], F.-J. Hambsch[10,11]

[1] INAF-Catania Astrophysical Observatory, via S.Sofia, 78 I-95123 Catania, Italy
e-mail: sergio.messina@oact.inaf.it
[2] Universitá di Catania, Dipartimento di Fisica e Astronomia, Sezione Astrofisica, via S. Sofia 78, I-95123 Catania, Italy
e-mail: a.lanzafame@unict.it
[3] Canada-France-Hawaii Telescope, 65-1238 Mamalahoa Hwy, Kamuela, HI 96743, USA
e-mail: malo@cfht.hawaii.edu
[4] INAF-Osservatorio Astronomico di Padova, Vicolo dell'Osservatorio 5, I-35122 Padova, Italy
e-mail: silvano.desidera@oapd.inaf.it
[5] Instituto de Astronomía y Física del Espacio (IAFE-CONICET), Buenos Aires, Argentina
e-mail: abuccino@iafe.uba.ar
[6] Departamento de Física, FCEN-Universidad de Buenos Aires, Argentina
[7] Department of Physics, College of Science, Guizhou University, Guiyang 550025, P.R. China
e-mail: liy_zhang@hotmail.com
[8] Research Institute Crimean Astrophysical Observatory, 298409, Nauchny, Crimea
e-mail: svetaartemenko@rambler.ru
[9] York Creek Observatory, Georgetown, Tasmania, Australia
e-mail: mervyn.millward@yorkcreek.net
[10] Remote Observatory Atacama Desert (ROAD), Vereniging Voor Sterrenkunde (VVS), Oude Bleken 12, B-2400 Mol, Belgium
e-mail: hambsch@telenet.be
[11] American Association of Variable Star Observers (AAVSO), Cambridge, MA, USA

ABSTRACT

Context. Low-mass members of young loose stellar associations and open clusters exhibit a wide spread of rotation periods. Such a spread originates from distributions of masses and initial rotation periods. However, multiplicity can also play a significant role.
Aims. We want to investigate the role played by physical companions in multiple systems in shortening the primordial disc lifetime, anticipating the rotation spin up with respect to single stars.
Methods. We have compiled the most extensive to date list of low-mass bona fide and candidate members of the young 25-Myr β Pictoris association. We have measured from our own photometric time series or from archival time series the rotation periods of about all members. In a few cases the rotation periods were retrieved from the literature. We used updated UVWXYZ components to assess the membership of the whole stellar sample. Thanks to the known basic properties of most members we built the rotation period distribution distinguishing between bona fide members and candidate members and according to their multiplicity status.
Results. We found that single stars and components of multiple systems in wide orbits (>80 AU) have rotation periods that exhibit a well defined sequence arising from mass distribution with some level of spread likely arising from initial rotation period distribution. All components of multiple systems in close orbits (<80 AU) have rotation periods significantly shorter than their equal-mass single counterparts. For these close components of multiple systems a linear dependence of rotation rate on separation is only barely detected. A comparison with the younger 13 Myr h Per cluster and with the older 40-Myr open clusters/stellar associations NGC2547, IC 2391, Argus, and IC 2602 and the 130-Myr Pleiades shows that whereas the evolution of F-G stars is well reproduced by angular momentum evolution models, this is not the case for the slow K and early-M stars. Finally, we found that the amplitude of their light curves is correlated neither with rotation nor with mass.
Conclusions. Once single stars and wide components of multiple systems are separated from close components of multiple systems, the rotation period distributions exhibit a well defined dependence on mass that allows to make a meaningful comparison with similar distributions of either younger or older associations/clusters. Such cleaned distributions allow to use the stellar rotation period as age indicator, meaningfully for F and G type stars.

Key words. Stars: activity - Stars: late-type - Stars: rotation - Stars: starspots - Stars: open clusters and associations: individual: beta Pictoris

1. Introduction

β Pictoris is a nearby young loose stellar association. Its members have an average distance from the Sun of about 40±17 pc and an age of about 25±3 Myr (Messina et al. 2016a; hereafter Paper I). Youth and proximity make this association a special benchmark in stellar astrophysics studies. In fact, the young age secures the presence of interesting circumstellar environments in many members, where discs and planetary systems can be discovered. The proximity allows to spatially resolve them giving effective possibility to study disc morphology and the planetary system's architecture. The A3V star β Pictoris, from which the association takes the name, is one such example (see, e.g., Chauvin et al. 2012). Youth, vicinity, and brightness of its members explain why this association has been included in many studies to search for very low-mass stellar and planetary companions, as well as to accurately measure element abundances, magnetic activity, and kinematics. Among many studies, we mention those aimed at searching for planetary companions and discs like the *SEEDS* project (Strategic Exploration of Exoplanets and Disks with Subaru; Brandt et al. 2014), *The Gemini/NICI planet-finding campaign* (Biller et al. 2013), *SPHERE* (Spectro-Polarimetric High-contrast Exoplanet REsearch, Beuzit et al. 2008), and *NaCo Large Program* (Desidera et al. 2015); those aimed at searching and characterizing new members, like *SACY* project (Search for Associations Containing Young stars; Torres et al. 2006, 2008; da Silva et al. 2009; Elliott et al. 2014), *The solar Neighborhood* investigation (Riedel et al. 2014), the *BANYAN* project (Bayesian Analysis for Nearby Young Associations; Malo et al. 2013, 2014a, 2014b), and many other membership investigations (see, e.g., Lépine & Simon 2009; Kiss et al. 2011; Schlieder et al. 2010, 2012; Shkolnik et al. 2012; Malo et al. 2013, 2014a, 2014b) resulting in a significantly increased number, by about a factor 3, of confirmed and new candidate members, with respect to the association members detected in discovery studies (e.g., Zuckerman et al. 2001).

The first comprehensive rotational investigation of the low-mass (spectral types F to M) members of the β Pictoris association was carried out by Messina et al. (2010, 2011). They measured the rotation periods of 33 on a list of 38 among confirmed and candidate members compiled from Zuckerman & Song (2004) and Torres et al. (2006, 2008).

The rotational properties of the β Pictoris association represent a key information for a number of studies concerning, e.g., the pre-main-sequence (PMS) angular momentum evolution of low-mass stars (see Spada et al. 2011; Gallet & Bouvier 2013, 2015), the effect of rotation on Lithium depletion at young ages (Pallavicini et al. 1993; Bouvier et al. 2016; Messina et al. 2016a), the impact of photoevaporation and binary encounters on the primordial disc life time (Olczak et al. 2010; Throop & Bally 2008) and the time scale of the star-disc locking phase, which can all be probed by means of the star's rotation (see, e.g., Messina et al. 2014, 2015a, 2015b), as well as the implication for the formation of planets around binaries (see, e.g., Alexander 2012).

Considering the importance of the β Pictoris association for these studies, the increased number of newly discovered members, and the fact that the basic properties of many members have been time by time better established (thanks to their brightness), we realized that the time was ripe for carrying out a new rotational study on this enlarged sample. The results of this extensive study were presented in the catalog of photometric rotational periods by Messina et al. (2016b; hereafter Paper II) containing the photometric rotational periods of 112 low-mass members and candidate members of the β Pictoris association. These rotation periods were used to explore the rotation-Lithium connection and to obtain an improved age estimate of the β Pictoris association using the Lithium Depletion Boundary method (Paper I). In the present study (Paper III), we aim at exploiting this catalogue of rotation periods to investigate the distribution of rotation periods versus mass and the role played by multiplicity, which is known for most members, in determining the wide spread of rotation periods observed in this and other young loose associations.

In Sect. 2, we present the up-to-date and most complete sample of members. In Sect. 3, we discuss on the basic properties, color and rotation period, that are used in our analysis. In Sect. 4, we present the results of our period search. In Sect. 5, we assess the membership of the whole sample using updated space and velocity components. In Sect. 6, we discuss the rotation period distribution and present new results on the impact of multiplicity on the rotation evolution. In Sect. 7, we make a comparison of the rotation period distribution with those of younger and of older open clusters and associations. Dependence of photospheric activity, as measured from light curve amplitude, on rotation and mass is discussed in Sect. 8. In Sect. 9, we give our conclusions.

2. Sample description

The present study is based on the catalog of photometric rotational periods of low-mass members and candidate members of the β Pictoris association presented in Paper II. Briefly, we have carried out an extensive search in the literature to retrieve all members of the β Pictoris association. We compiled a list of 117 among bona fide and candidate members, with spectral types later than about F3V, from the following major studies: Torres et al. (2006, 2008), Lépine & Simon (2009), Kiss et al. (2011), Schlieder et al. (2010, 2012), Shkolnik et al. (2012), Malo et al. (2013, 2014a, 2014b), and other studies detailed for each member in Paper II. Stars of earlier spectral types were excluded from our sample since the photometric rotation period to be measured requires the presence of a detectable level of magnetic activity (more specifically, of light rotational modulation by surface temperature inhomogeneities with amplitude of several millimag at least). This circumstance generally occurs in late spectral type stars that have an external convection zone, which allows for the production of magnetic fields and is subjected to magnetic braking.

We measured the rotation periods of 112 out of 117 stars either from our own photometric monitoring or from photometric time series in public archives, or we retrieved these periods from the literature.

Information on individual stars either from our own analysis or from the literature and references can be retrieved in Paper II. Information on the membership is not homogeneous for all the targets either for the number

Send offprint requests to: Sergio Messina

⋆ Tables 2-3 are only available in electronic form at the CDS via anonymous ftp to cdsarc.u-strasbg.fr (130.79.128.5) or via http://cdsweb.u-strasbg.fr/cgi-bin/qcat?J/A+A/.

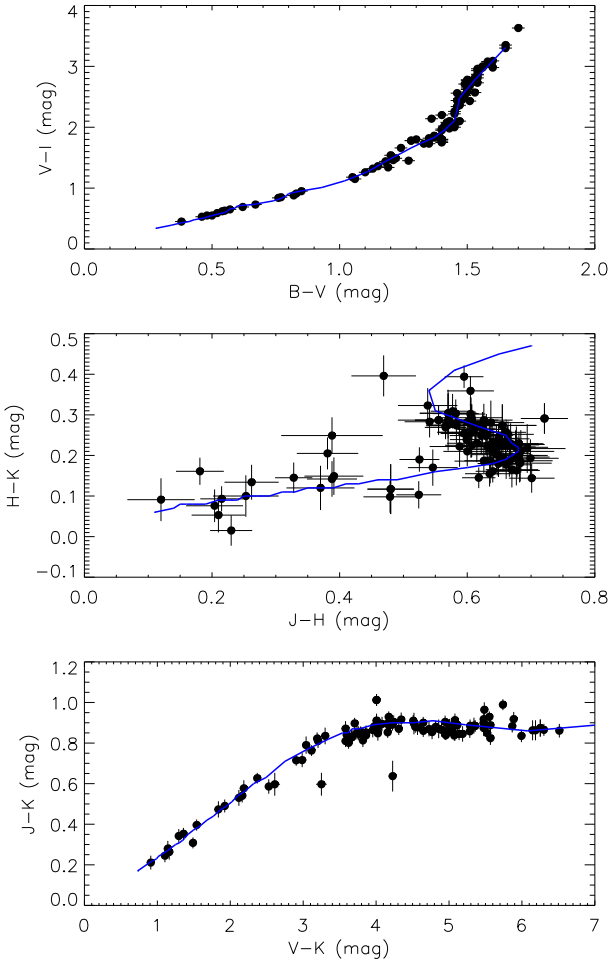

Fig. 1 Color-color plots for the β Pictoris members and candidate members with overplotted polynomial fits to the corresponding colors taken from Table 6 of Pecaut & Mamajek (2013).

of studies or for the methods. For example, we found more than four membership studies for 52 targets, whereas only one membership study for 15 targets. For this reason, in Sect. 4, we present the results of our membership study based on updated space and velocity components and Lithium equivalent width (EW).

The single/binary nature of our targets is based on the available RV measurements and direct imaging studies, which are referenced for each target in Appendix A of Paper II. We note that not all stars with constant RV have been observed with high-contrast direct imaging. Therefore, for these stars, despite the RV constancy, we cannot rule out the presence of a wide orbit companion. However, even if this is the case, their rotational properties are indistinguishable from those of known wide binaries (see Sect. 5). Targets with not determined either single or binary nature from RV studies are flagged with a symbol '?' in the last column of Table 1. The complete target's list is reported in Table 1.

3. Target properties

3.1. Colors

Our aim is to investigate the distribution of the rotation periods versus stellar mass and the impact of multiplicity on the observed rotation period spread. The stellar mass for the majority of our target stars has to be derived from a comparison with evolutionary mass tracks at the age of the β Pictoris association. The derived masses, especially for later spectral type stars, significantly depend on the adopted model, with models including effects of magnetic fields giving results more congruent with other age dating methods with respect to non magnetic models (see, Messina et al. 2016c for a detailed discussion). The associated uncertainty on the mass value derives from the uncertainties on distance, apparent magnitude, and effective temperature. In most cases, effective temperatures, which are inferred from spectral types especially for the mid- to late-M stars, have uncertainties not smaller than $\pm$100 K. For this reason, we have investigated which color index is the best stellar mass proxy.

In our sample, B−V and V−I are available for 60 targets; 41 targets have V−I only; 6 targets have B−V only. All these colors are listed in Table 1 of Paper II and were compiled from different sources in the literature. The remaining 10 targets have both B−V and V−I colors unknown. Since the color is a basic parameter in the following analysis, we had to recover the missing values. In the top panel of Fig. 1, we plot the observed V−I versus B−V colors for the program stars. We overplot (blue solid line) a polynomial fit to the intrinsic V−I versus B−V colors listed by Pecaut & Mamajek (2013) for the 5–30 Myr old stars. The agreement is good with an average scatter of 0.05 mag of our colors from the polynomial relation. The agreement mainly arises from the fact that there are a number of β Pictoris members in our sample that were used by Pecaut & Mamajek to infer their tabulated colors for young stars. We used this relation to derive the colors from the measured V−I and B−V colors, respectively, for the mentioned targets missing either B−V or V−I, and their associated uncertainty is 0.05 mag. For the remaining 10 targets with no colors, we inferred them from the spectral type using again the Pecaut & Mamajek color versus Spectral Type relations, with an associated uncertainty of 0.07 mag. For instance, the distances of our targets have an average value of about 40 pc, therefore, the interstellar reddening can be considered negligible and we did not apply any color correction in our analysis.

We note that whereas the B−V color index of our targets spans a range $\Delta\sim$1.35 of magnitudes, the V−I color index spans a much larger $\Delta\sim$3.3 magnitude range, then the latter color index is better suited to represent stars of different masses. On the other hand, in addition to the limit arising from the use of derived V−I colors for about $\sim$70% of the sample, the two colors come from different works for the majority of stars and they were measured at different epochs. Due to magnetic activity, colors can vary in time up to several hundredths of magnitude[1] in such a young association. Therefore, the measured colors (and those de-

[1] The series of papers on the multiband photometric monitoring of active stars by Cutispoto et al. (e.g., 2003, and references therein), provide an exhaustive example.

rived) are not as homogeneous as we would like.

In the middle panel of Fig. 1, we plot the H−K_s versus J−H colors of our targets measured by the 2MASS project (Cutri et al. 2003). We overplot (blue solid line) a polynomial fit to the intrinsic H−K_s versus J−H colors listed by Pecaut & Mamajek (2013) for the 5–30 Myr old stars. We note that a few stars deviate significantly from this relation. They are close binaries with components of different spectral types that were unresolved by 2MASS. We note that the 2MASS color indices of our targets span a range of magnitudes not larger than $\Delta\sim0.6$, which is too small for our purposes, and, more importantly, the relation is not univocal.
Finally, in the bottom panel of Fig. 1, we plot the J−K_s versus V−K_s colors of our targets measured by 2MASS, whereas the V magnitude is the one listed in Table 1 of Paper II and taken (for 98 out of 117 stars) as the brightest (and presumably unspotted) magnitude in the ASAS (All Sky Automated Survey; Pojmanski 1997) timeseries or as the brightest magnitude reported in literature (for the remaining 19 stars). Again, we note a few stars deviating significantly from the average trend. We find that the V−K_s color index has a magnitude range of $\Delta\sim7$ and is the best suited to investigate the color-period distribution. The use of the V−K_s color allows us to deal with an average uncertainty from ∼2% for K0V stars to less than ∼0.5% for late-M stars.

For instance, we note that a comparison with the polynomial fit from Pecaut & Mamajek (2013) shows that our targets that belong to multiple systems and are unresolved in the 2MASS photometry (separation $\rho \leq 6''$ between the components) have V−K_s colors redder on average by 0.03 mag with respect to resolved targets.

3.2. Rotation period

The other fundamental stellar property in our investigation is the rotation period. To measure the photometric rotation periods of our targets, we used archive data, we made use of periods from the literature, and carried out our own multi-observatory observations. A detailed description of the instruments, log of the observations, and information on data reduction and analysis, and the results of the period search are presented in Paper II.
Briefly, in our sample, 52 stars have photometric time series in one or more of the following public archives: ASAS (All Sky Automated Survey; Pojmanski 1997), SuperWASP (Wide Angle Search for Planets; Butters et al. 2010), Integral/OMC (Domingo et al. 2010), Hipparcos (ESA 1997), NSVS (Northern Sky Variability Survey; Woźniak et al. 2004), MEarth (Berta et al. 2012), and CSS (Catalina Sky Survey; Drake et al. 2009). We have retrieved and analysed all the available time series for the period search.
Another 20 stars in our sample had no archive data and, thus, they were photometrically monitored by us for the first time. We also observed another 15 stars that, although present in one of the mentioned archives, were either in close binary systems with unresolved components or the archive data did not allow a period determination. We obtained either photometric time series for the resolved components or photometric series suitable for a successful period measurement. For the remaining 30 stars we adopted the rotation periods available in the literature. The results are summarized in Table 2 of Paper II.
To search for the stellar rotation periods of our targets we have followed an approach similar to that used in Messina et al. (2010, 2011). We refer the reader to those papers and to Paper II for a detailed description of the methods.
As a result of our photometric analysis, we obtained the rotation period of 112 out of 117 target stars. Specifically, we measured for the first time the rotation period of 56 stars. For another 27 stars, we confirmed the values reported in the literature with our analysis of new or archived data. For 29 stars we adopted the literature values. For the remaining 5 stars, our periodogram analysis did not provide the rotation period.

4. Membership assessment

For a meaningful investigation of the rotation period distribution and dependences on multiplicity, we first carried out a membership assessment of all 117 stars in our sample by comparing their Galactic velocity (UVW)[2] relative to the Sun and space (XYZ) components with respect to the association average values. The proper motions, radial velocities, and distances used to derive UVW and their uncertainties, and XYZ are listed in Table 2 together with their references. We generally found more measurements of RV for each star in the literature and measured a weighted average and its standard deviation for our purposes. Individual RV measurements and relative references are listed in Table 3.
To measure the average values of the Galactic components, we selected an initial sub-sample consisting of stars that were already known as bona fide members of the association and, more precisely, that were investigated in several earlier studies (up to eight for a few; see Paper II) that all agreed to assign the membership to the β Pictoris association.
Among these stars, we subsequently selected only single and wide-orbit components of multiple systems to minimize the effect on the derived Galactic components of RV variation arising from orbital motion. In such a way, we were left with 41 stars that represent our 'core' sample.
We use this core sample to compute the average $\overline{U}$, $\overline{V}$, and $\overline{W}$ velocity components and their standard deviations σ_U, σ_V, and σ_W, and the average $\overline{X}$, $\overline{Y}$, and $\overline{Z}$ space components and their standard deviations. After computing average values and standard deviations, we found six stars of the core sample that significantly deviated ($> 3\sigma$) from the other core members in two of three planes ([U,V], [U,W],[V,W]): four components of wide binaries (2MASS J02014677+0117161, RBS 269, 2MASS J04435686+3723033, TYC 6872 1011 1), and two single stars (2MASS J02175601+1225266, 2MASS J16430128-1754274 with very large uncertainties in their velocity components). These stars were excluded from the core sample and new average values and standard deviations were recomputed as reported in the following:

$$\overline{U}(km\,s^{-1}) = -10.27 \pm 1.68 \quad (1)$$

[2] U positive towards the Galactic center, V positive in the direction of the Galactic rotation, and W positive in the direction of the Galactic north pole.

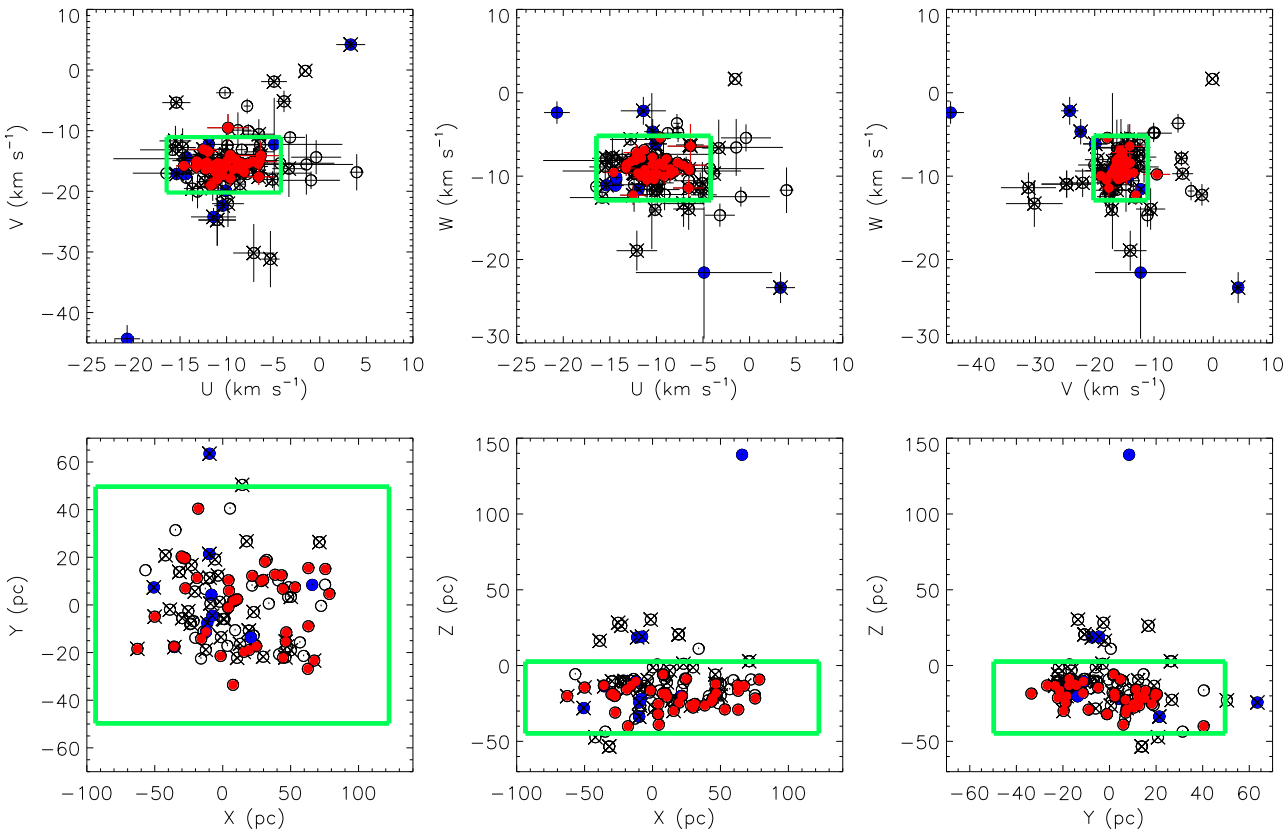

Fig. 2 Distribution of UVW velocity (top panels) and XYZ space (bottom panels) Galactic components of members and candidate members of the β Pictoris association. Red bullets represent the core sample, open bullets the candidate members, blue bullets the rejected members, crossed symbols are stars with no Li measurement. The green rectangular boxes identify the plane region within 3σ from the average values (see text).

$$\overline{V}(km\,s^{-1}) = -15.80 \pm 0.90 \quad (2)$$

$$\overline{W}(km\,s^{-1}) = -8.77 \pm 1.20 \quad (3)$$

$$\overline{X}(pc) = 18 \pm 32 \quad (4)$$

$$\overline{Y}(pc) = 1 \pm 16 \quad (5)$$

$$\overline{Z}(pc) = -20 \pm 7 \quad (6)$$

In Fig. 2, we show the 6D kinematic distributions of all 117 stars in our sample. Red bullets represent our core members and the rectangular boxes identify the plane region within 3σ from the average values. The values we derived are in agreement within the uncertainties with the values of Torres et al. (2008).
In addition to the kinematics, we used also the Li EW, whenever available (see Paper I for a list of targets with measured Li EW), as a strong constrain to asses the membership. Those stars in our sample whose UVW and XYZ differ by less than 3σ from the average values of the core sample but whose Li EW significantly deviates ($>3\sigma$) from the linear fits to the distribution exhibited by core members (see Fig. 2 in Paper I) are considered non members of the association.

The results of our membership assessment are summarized in Table 4. As result, in our sample we have 80 bona fide members (flagged with 'Y'), of which 35 constituting the core sample (flagged with 'Core'), that fully satisfy our criteria for membership, and the above mentioned six bona fide members as reported in the literature, but excluded from our core sample (flagged with 'Core_e'). In the present study, we classify as candidate members those stars that have from one to three among space and velocity components deviating more than 3σ from the average of the β Pictoris association. Whereas, we classify as non members those stars with more than three among space and velocity components deviating more than 3σ from the average. Accordingly, in our sample we have 22 candidate members (flagged with 'C') and 15 non members (flagged with 'NO'). We note that in the following the adjectives 'bona fide' and 'candidate' only refer to the membership status and not to the single/multiple nature of the targets.

5. Discussion

It is unanimously accepted that most if not all low-mass stars form with an accretion protostellar disc that, at early stages, magnetically locks the central star to an about constant angular velocity (e.g. Shu et al. 2000). The disc life-

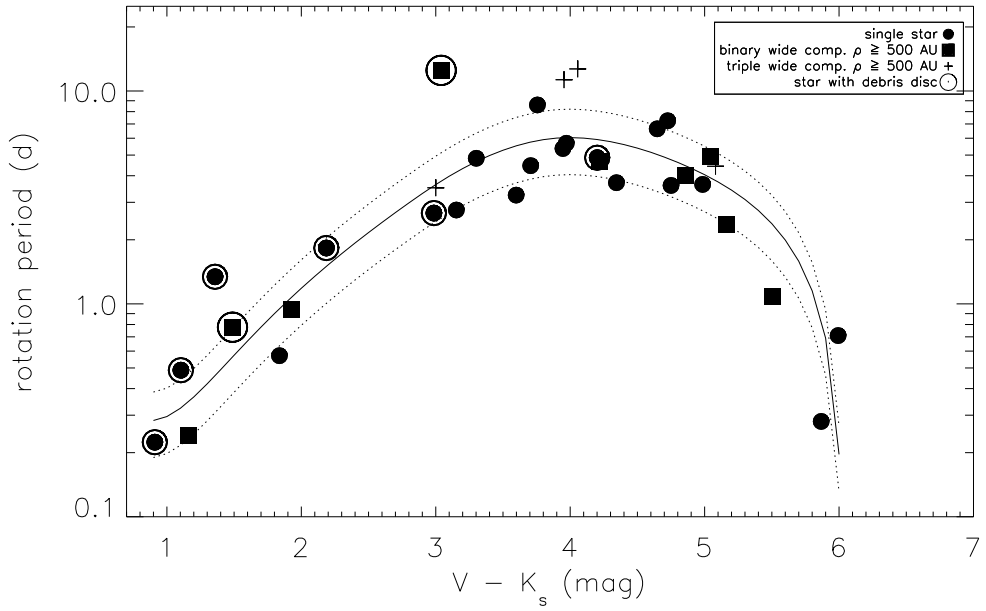

Fig. 3 Distribution versus V−K_s color of the rotation periods of the β Pictoris bona fide members that are either single (21 stars) or wide ($\rho > 500$ AU) components of binary/multiple systems (14 stars). The meaning of the symbols is given in the legend. The solid line is a polynomial fit to the rotation periods. Dotted lines represent the $\pm 3\sigma$ standard deviation of the residuals with respect to the fit.

time has a range of values and stars with a long-lived disc reach the Zero Age Main Sequence rotating more slowly than stars with a short-lived disc. Theories predict that the protostellat disc lifetime can be significantly shortened if a binary companion is present, which can truncate the disc, reducing the efficacy of the PMS disc-locking (Meibom et al. 2007, Bouvier et al. 1993, Edwards et al. 1993, Ingleby et al. 2014, Rebull et al. 2004), enhancing the mass accretion (Papaloizou & Terquem 1995), and finally disrupting the disc (Artymowicz 1992). In this circumstance, the amplitude of the perturbation should be related to the separation between the components. These predictions are confirmed by observational studies, e.g. by Kraus et al. (2016) and Cieza et al. (2009), who found that stars without IR excess tend to have companions at smaller separation than stars with excess indicating the presence of a disc. Both studies find that the depletion of protoplanetary discs among binary systems with components closer than 40 AU is a factor 2 larger than in either single or wide binaries already at age as young as 1-2 Myr. Moreover, if present, discs around close components (< 30 AU) of binary systems have disc mass depleted by a factor 25 with respect to single stars. The impact of a short-lived discs on rotation in binary systems is also documented by, e.g., Stauffer et al. (2016) who report that photometric binaries among the Pleiades GKM-type stars tend to rotate faster than their counterpart single stars, with an effect that is more pronounced among equal-mass binaries than in single-line spectroscopic binaries; or by Douglas et al. (2016) who report that most, if not all, rapid rotators that deviate from the single-valued relation between mass and rotation already reached by the age of the Hyades, belong to multiple systems.

We are now in the position to extend this investigation of the effect of multiplicity on rotation period distribution towards a much younger age of 25 Myr, using our sample of β Pictoris members and candidate members whose single/multiple nature is well characterized. Moreover, in a sparse system like the β Pictoris association, one can assume that stellar encounters have a minor role in altering the stellar angular momentum evolution via disc dissipation or enrichment. Moreover, in the absence of nearby massive stars, disc photo-evaporation by external UV radiation can also be ignored.

We intend to verify that multiplicity really affects the rotational properties and identify the projected separation at which the components of binary/multiple systems of the β Pictoris association start to exhibit rotation periods that significantly deviate from the period distribution of single stars.

5.1. Period distribution of bona fide members

5.1.1. Single stars and components of binary/multiple systems

We start our analysis considering only bona fide members that are single stars and wide components of multiple systems sufficiently distant from each other (projected separation $\rho > 500$ AU) to secure that their rotation periods can be considered as they were single stars. In the following, we will show that separations down to 80 AU do not affect significantly the observed rotation periods.

Then, we selected 35 stars: 21 single stars and 14 wide components of multiple systems with $\rho > 500$ AU (Fig. 3). These stars have rotation periods that exhibit the following mass dependence: the rotation period increases towards lower masses (redder colors) reaching a maximum at V−K_s

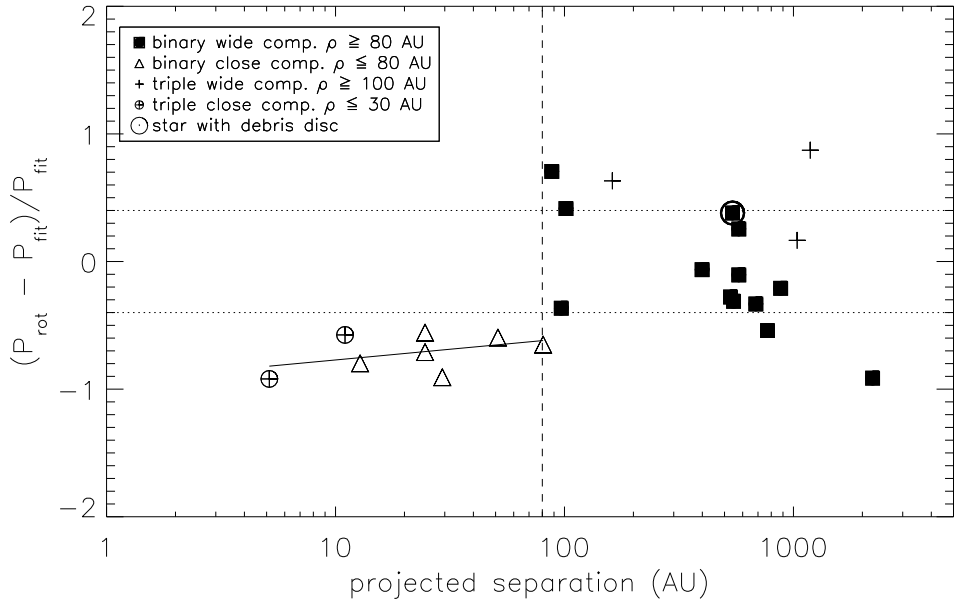

Fig. 4 Relative residuals versus projected separation (AU) of the rotation periods of all bona fide members in binary/multiple systems with respect to the polynomial fit (solid line in Fig. 3). The meaning of the symbols is given in the legend. We note that in our sample there are no components of triple systems with separation in the range 30–100 AU.

$\simeq 4$ mag, then decreases towards the very-low-mass regime. To measure the mass dependence of the rotation period, we proceeded as follows. We computed the median periods over color bins of 1 mag and computed a polynomial fit to these median values (the solid line in Fig. 3) valid in the color range $0.9 < \mathrm{V{-}K}_s < 6$ mag and whose coefficients are given in Table 5. We find that the relative residuals with respect to the polynomial fit have a normal distribution with a standard deviation $\sigma = 0.11$. The dotted lines represent the $\pm 3\sigma$ standard deviation from the fit[3]. The existence of such a dispersion tells us that the rotation periods of single stars and wide components, in addition to the mass, also depend on other factors such as, for example, differences in the initial rotation periods.

The fit represents empirically the mass dependence of the rotational period of single stars and wide components of binary/multiple systems. The relative residuals $(\mathrm{P_{rot}} - \mathrm{P_{fit}})/\mathrm{P_{fit}}$ with respect to this fit can help us to identify which stars deviate significantly and to estimate empirically the minimum separation between the components of a system for which there is no significant departure from this fit. These relative residuals are plotted versus the projected separation (in AU) in Fig. 4. After excluding single stars and very wide components of multiple systems ($\rho > 5000$ AU), and the spectroscopic binaries that will be discussed separately, we find that the components of multiple systems with a projected separation $\rho \gtrsim 80$ AU are mostly within the $\pm 3\sigma$ distribution of single stars, therefore they behave like they were single stars. On the contrary, all components of multiple systems with a projected separation $\rho \lesssim 80$ AU deviate by more than 3σ. For these residuals, we find a linear Pearson correlation coefficient $r = 0.94$ with a significance level $\alpha > 99.5\%$ suggesting that the smaller the separation between the components the faster their rotation period with respect to equal-mass single stars, i.e., their rotation periods are significantly affected/shortened. However, the slope of the linear fit to the distribution of residuals for projected separations $\rho \lesssim 80$ AU

$$y = -0.87(\pm 0.24) + 0.20(\pm 0.19) \times log_{10}(\rho) \qquad (7)$$

where $y = (\mathrm{P_{rot}} - \mathrm{P_{fit}})/\mathrm{P_{fit}}$ (solid line in Fig. 4), has a relatively high uncertainty. Therefore, owing to the paucity of data so far available, we prefer to be more conservative and to state that all components of multiple systems with a projected separation $\rho \lesssim 80$ AU rotate significantly ($>3\sigma$) faster, but a linear dependence of rotation rate on separation is only barely detected.

Among the wide components ($\rho \gtrsim 80$ AU) we note four stars[4] (all core members) that deviate more than 3σ from the general trend exhibited by the majority of stars. Their departure probably indicates that our scenario, where the separation between the components is the dominant parameter that differentiates the period evolution from that of single stars, is a simplification. There are likely other factors that, in individual cases, can be even more important than the separation.

In Fig. 5, we plot the rotation periods versus $\mathrm{V{-}K}_s$ colors of all bona fide members of the β Pictoris association (not only those at $\rho > 500$ AU as in Fig. 3). In addition to the six mentioned stars (see footnotes 3 and 4), also

[3] We excluded from the fit HIP 11437A ($\mathrm{V{-}K}_s = 3.04$ mag; P = 12.5 d) and HD 160305 ($\mathrm{V{-}K}_s = 1.36$ mag; P = 1.341 d) because of their significant ($>20\sigma$) departure from the general color-period trend.

[4] TYC 6878 0195 1: $\mathrm{V{-}K}_s = 2.90$ mag and P = 5.70 d; BD−211074A: $\mathrm{V{-}K}_s = 4.35$ mag and P = 9.3 d; TYC 7443 1102 1: $\mathrm{V{-}K}_s = 3.95$ mag and P = 11.3 d; TX Psa: $\mathrm{V{-}K}_s = 5.57$ mag and P = 1.080 d.

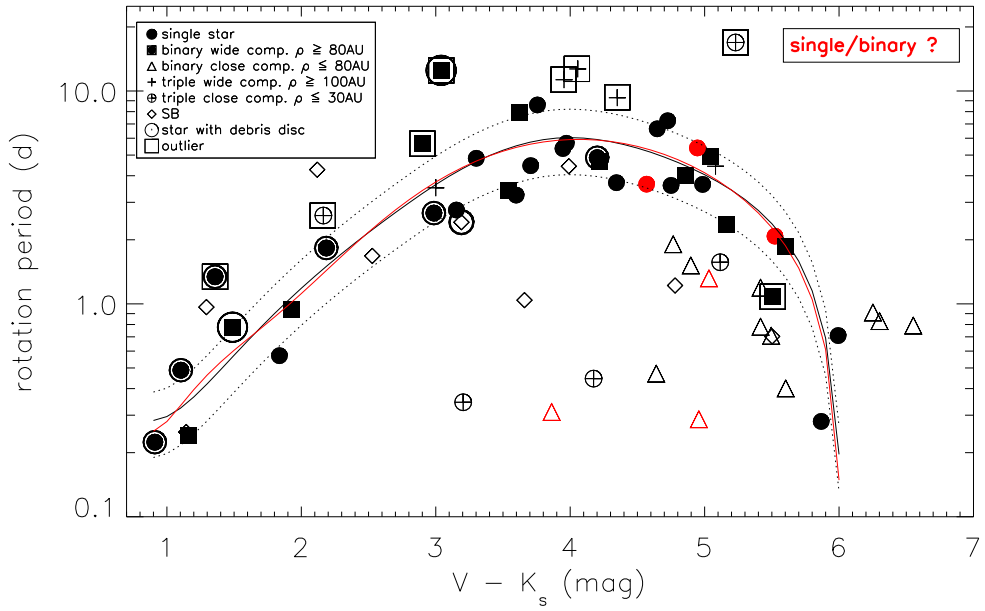

Fig. 5 The same as in Fig. 3, but with all the bona fide members of the β Pictoris association. Open squares indicate the members whose rotation periods significantly deviate either from the general trend exhibited by single stars and components of wide binaries (their residuals from the fit are $>3\sigma$) or from the distribution of visual close binaries. Red color is used for members whose single/binary nature is not know. We note the segregation of all close binaries at rotation periods shorter than the period distribution of single and wide components of multiple systems.

Table 5 Coefficients and uncertainties of the polynomial fit to the color-period distribution among bona fide members that are single stars and wide ($\rho > 500$ AU) components of multiple systems in the color range $0.9 < V-K_s < 6$ mag.

a0	a1	a2	a3	a4	a5	a6	a7	a8
8.38	−30.90	46.59	−36.37	16.16	−4.14	0.60	−0.046	0.00140
±1.75	±5.09	±5.99	±3.73	±1.36	±0.30	±0.04	±0.002	±0.00008

2MASS J20013718-3313139 ($V-K_s$ = 4.06 mag; P = 12.7 d), 2MASS J06131330-2742054 ($V-K_s$ = 5.23 mag; P = 16.9 d), and TYC 8742 2065 1 ($V-K_s$ = 2.16 mag; P = 2.60 d) deviate significantly from the general color-period trend exhibited by the other members. The existence of these outliers reminds us that in individual cases other factors apart from mass, component's separation, and initial rotation period, may play a significant role in driving the rotational evolution.

5.1.2. Spectroscopic binaries

Our stellar sample totals nine spectroscopic binaries (SBs) that are bona fide members (one of which, TYC 7408 0054 1, is an eclipsing binary). Five SBs have known both the components' separation and the orbital periods, which are all shorter than 5 days and about synchronized with the rotation period of their primary components (the differences amount to a few percents). The star HIP 23418 with a rotation period of P = 1.22 d against an orbital period P = 11.9 d represents the only exception. Considering the small ($\rho < 0.3$ AU) component's separation and the about orbital/rotation synchronization, we infer that tidal dissipation has been effective in these stars, as expected from tidal theory (see, e.g. Zahn 1977; Witte & Savonije 2002) and as supported by observational studies (see, e.g. Meibom et al. 2007). The tidal dissipation makes their angular momentum evolution different from that of single stars or wide components of binary systems. Considering that the remaining four SBs have same age (being bona fide members), similar total masses, and rotation periods shorter than 5 days, we may suppose that they also are likely significantly affected by tidal dissipation. Because we are focusing our analysis on effects on angular momentum evolution other than tidal dissipation, and the rotation periods of our SBs are not immediately comparable with those of the other stars in our sample, all SBs, but HIP 23418, are excluded from our analysis.

We have only three bona fide members in the very-low-mass regime ($V-K_s \geq 6.0$ mag) that are too red to be compared to the polynomial fit. This part of our color-period diagram is not enough populated to infer any reliable properties.

Finally, in our sample of bona fide members there are six stars (plotted with red symbols) whose single/binary nature is still not determined. We note that 2MASS J08173943-8243298 ($V-K_s$ = 5.03 mag; P = 1.318 d), 2MASS J17150219-3333398 ($V-K_s$ = 3.86 mag; P = 0.3106 d), and 2MASS J23500639+2659519 ($V-K_s$ = 4.96 mag; P = 0.287 d) occupy the region of the color-period diagram of close binaries, whereas 2MASS 05015665+0108429 ($V-K_s$ = 5.52 mag; P = 2.08 d), 2MASS J13545390-7121476 ($V-K_s$ = 4.57 mag; P = 3.65 d) and 2MASS J18420694-5554254 ($V-K_s$ =

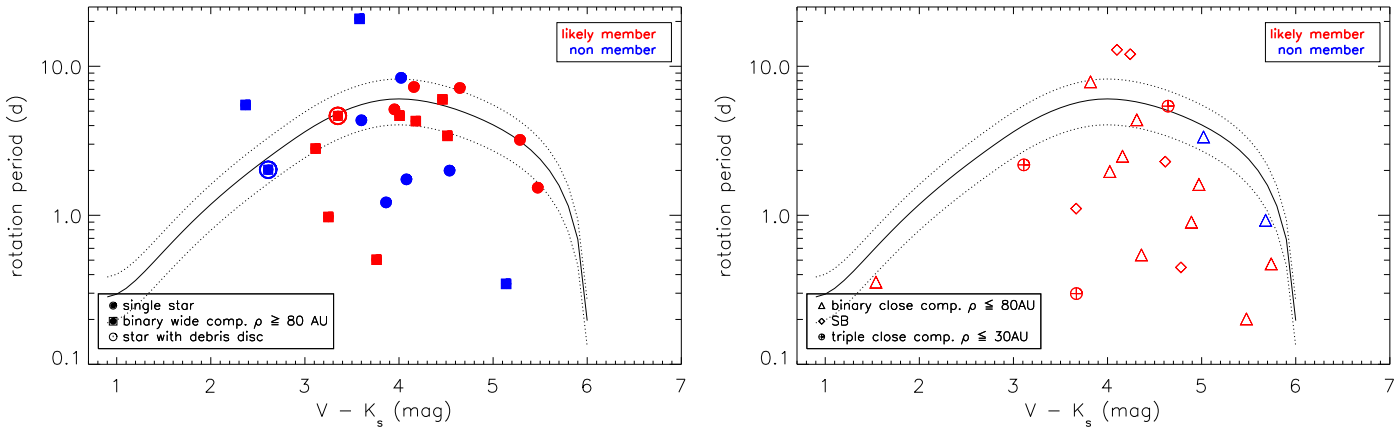

Fig. 6 The same as in Fig. 5, but for candidate members (red symbols) of the Association and non members (blue symbols). In the left panel we consider single stars and wide components of binary systems; in the right panel we consider the close components of binary systems and spectroscopic binaries.

4.95 mag; P = 5.403 d) occupy the region of the color-period diagram of single stars and wide components.

To summarize, the rotation periods of single stars and wide components of multiple systems with separation $\rho \gtrsim$ 80 AU exhibit a well defined mass dependence at the age of about 25 Myr that can be approximated by a polynomial fit with a dispersion not larger than a factor two. Only 9 bona fide members (marked with open squares in Fig. 5) out of 73 (excluding spectroscopic binaries and very-low mass stars) significantly deviate from the general color-period trend exhibited by the other members. The rotation periods of close components of multiple systems with separation $\rho \lesssim 80$ AU are all shorter and thus populate the region of the color-period diagram below the distribution of single stars and wide components. When the single/binary nature of the cluster or association members is taken into account, the period distribution even at young ages, like the presently considered 25 Myr, has a spread much smaller than claimed in earlier studies.

5.2. Period distribution of candidate members

The sample of bona fide members has allowed us to discover that single stars and wide components of binary/multiple systems have a period distribution different than that of components of close binary/multiple systems. We can take advantage of such a different behavior to infer some hint on the candidate members.

5.2.1. Single stars

In our sample there are five single candidate members, which are plotted as red bullets in the left panel of Fig. 6. These candidates have some kinematics component larger than 3σ but their rotation periods fit well into the color-period distribution of single bona fide members. We consider these stars as likely members of the association. These stars are 2MASS J16572029-5343316 (V−K$_s$ = 4.65 mag; P = 7.15 d), 2MASS J23512227+2344207 (V−K$_s$ = 5.29 mag; P = 3.208 d), 2MASS J16430128-1754274 (V−K$_s$ = 3.95 mag; P = 5.14 d, which was excluded from the core sample), TYC 5853 1318 1 (V−K$_s$ = 4.16 mag; P = 7.26 d), and 2MASS J05294468-3239141 (V−K$_s$ = 5.47 mag; P = 1.532 d).
In the left panel of Fig. 6, we also plot the five single stars that are non members (blue bullets). The rotation periods of three of them deviate significantly from the distribution. However, the rotation periods of TYC 915 1391 1 (V−K$_s$ = 3.60 mag; P = 4.34 d) and 2MASS J20055640-3216591 (V−K$_s$ = 4.02 mag; P = 8.368 d), although non members, fit well into the distribution. This circumstance poses a severe caveat to the use of the rotation period when inferring the age of individual stars. That is, the fact that the rotation period of a single star fits well into the period distribution of the association is a necessary but not sufficient condition to be classified as member.

5.2.2. Wide components of binary/multiple systems

Similarly, in our sample there are seven candidate members that are wide components of multiple systems (red squares). These candidates have some kinematics component larger than 3σ but the rotation periods of six of them fit well into the color-period distribution of single bona fide members. We consider these stars as likely members of the association. These stars are 2MASS J02014677+0117161 (V−K$_s$ = 4.51 mag; P = 3.41 d), and RBS 269 (V−K$_s$ = 4.46 mag; P = 6.0 d), which were excluded from the core sample, 2MASS J04435686+3723033 (V−K$_s$ = 4.18 mag; P = 4.288 d), 2MASS J18202275-1011131A (V−K$_s$ = 3.35 mag; P = 4.655 d), 2MASS J18202275-1011131B (V−K$_s$ = 4.01 mag; P = 5.15 d), and TYC 1208 0468 1 (V−K$_s$ = 3.11 mag; P = 2.803 d). For this star, however, we note that the rotation period is shorter than that of other members with similar separation (∼100 AU) (see also Fig. 7).
The exception is represented by BD+262161B (V−K$_s$ = 3.25 mag; P = 0.974 d) and TYC 6872 1011 1 (V−K$_s$ = 3.76 mag; P = 0.503 d, which was excluded from the core sample) whose rotation periods are in disagreement with the distribution.

In the left panel of Fig.6, we also plot the five non member wide components (blue squares): the following stars have accordingly their rotation period in disagreement with

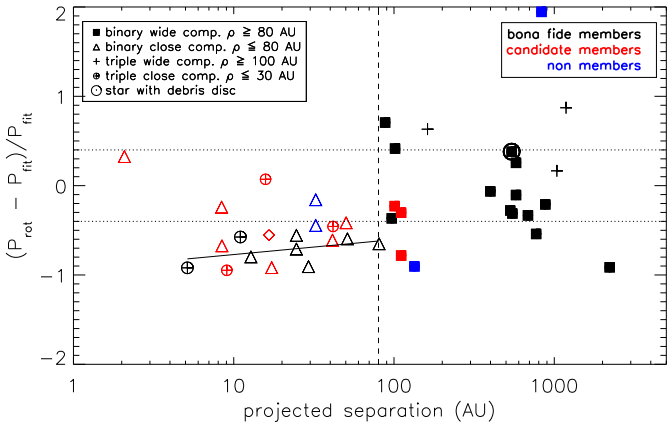

Fig. 7 The same as in Fig. 4, but with inclusion of candidate members and non members.

the distribution, that is 2MASS J01365516-0647379 ($V-K_s$ = 5.14 mag; P = 0.346 d); HIP105441 ($V-K_s$ = 2.37 mag; P = 5.50 d); and TYC 9114 1267 1 ($V-K_s$ = 3.58 mag; P = 20.8 d). An exception is represented by the debris disc BD +26 2161A ($V-K_s$ = 2.61 mag; P = 2.022 d) whose rotation period is in agreement with the distribution.

5.2.3. Close components of binary/multiple systems

In the right panel of Fig. 6, we plot the 9 components of close binary systems that are candidate members (red triangles). They all but one exhibit rotation periods that are below the distribution of single and wide components, similarly to close components that are bona fide members. However, differently than single stars, this information is not a strong constraint to the membership. For these stars we can state that their rotation period is in agreements with the distribution of the members. However, this is a necessary but not sufficient condition to be considered members. There are other association/clusters with different ages whose period distribution significantly overlap at these short rotation regimes. The only exceptions are HIP 50156 and BD -21 1074B whose rotation periods are too long with respect to the close components members of the β Pictoris association. We plot also the three close binary non members (blue triangles), which exhibit rotation periods that tend to be too long and in disagreements with the distribution of the close binary members.

5.2.4. Spectroscopic binaries

Our stellar sample totals four spectroscopic binaries that are candidate members (red diamonds). We have information neither on orbital period nor on component's separation. Also their age is not definite, according to their candidate status. Therefore, we are not in position to infer if their angular momentum has suffered or not significant tidal dissipation. As in Sect. 5.1, we exclude them from our analysis.

In Fig. 7, we plot the period residuals with respect to the fit versus the projected separation, as in Fig. 4, of all bona fide members, candidate members and non members. As shown by the red color, those stars that we classified as likely members follow the distribution exhibited by bona fide members. Our investigation, therefore, supports their candidate membership of the β Pictoris association. On the contrary, the following candidate members: HIP 50156 (ρ = 2.08 AU; $(P_{rot} - P_{fit})/P_{fit}$ = 0.325), BD -21 1074B (ρ = 15.79 AU; $(P_{rot} - P_{fit})/P_{fit}$ = 0.071), BD +26 2161B (ρ = 110.7; $(P_{rot} - P_{fit})/P_{fit}$ = -0.78); TYC 4770 0797 1 (ρ = 8.4 AU; $(P_{rot} - P_{fit})/P_{fit}$ = -0.24), do not follow the general trend and our study suggests their non membership.

To summarize, the rotation period represents a valuable information when assessing the membership of a star provided that its single/multiple nature and, in the latter case, the separation between the components, are known. The good fitting of the rotation period into the distribution of a proposed association/cluster is a necessary condition for the star to be member, although the rotation period alone does not provide a sufficient condition.

5.3. Wide components of triple systems

We note that the wide components of triple systems tend to have rotation periods comparable to but slower than either single stars or components of wide binaries. It seems that in these multiple systems, the initial angular momentum of the protostellar cloud, since divided among more components, may have given a fraction of it to the wide component, at least, smaller than what happens in case of binary systems.

The analysis presented in this Section shows that, when studying the stellar angular momentum evolution using the rotation period distributions of associations and open clusters, it is fundamental to know the single/binary nature of each member since their rotational properties are significantly different. Mixing single/wide components of multiple systems together with components of close binaries has the consequence to mask the real period segregation between these two different classes of stars, to make the rotation spread to appear larger than it is, and to bias the mean/median/percentile periods of a given cluster towards smaller values.

6. Comparison with other open clusters/associations

A study of the rotation period distribution of the β Pictoris members in the context of the angular momentum evolution is out of the scope of this paper. Nonetheless, a comparison with the rotation period distribution of other associations/clusters of different ages is very useful to infer some preliminary and qualitative results, at least, to be further developed elsewhere.
The more recent studies (see, e.g., Messina et al. 2016a) point towards ages of the β Pictoris association from 21 to 26 Myr. These estimates are significantly older than the estimates made by, e.g., Zuckerman et al. (2001) and Song et al. (2003), but, for instance, closer to the very first estimate provided by Barrado y Navascués et al. (1999).
The open cluster h Persei (Moraux et al. 2013) with an age of about 13 Myr and the open clusters/associations NGC 2547 (Irwin et al. 2008), IC 2391, Argus (Messina et al. 2011), and IC 2602 (Barnes et al. (1999)) with an

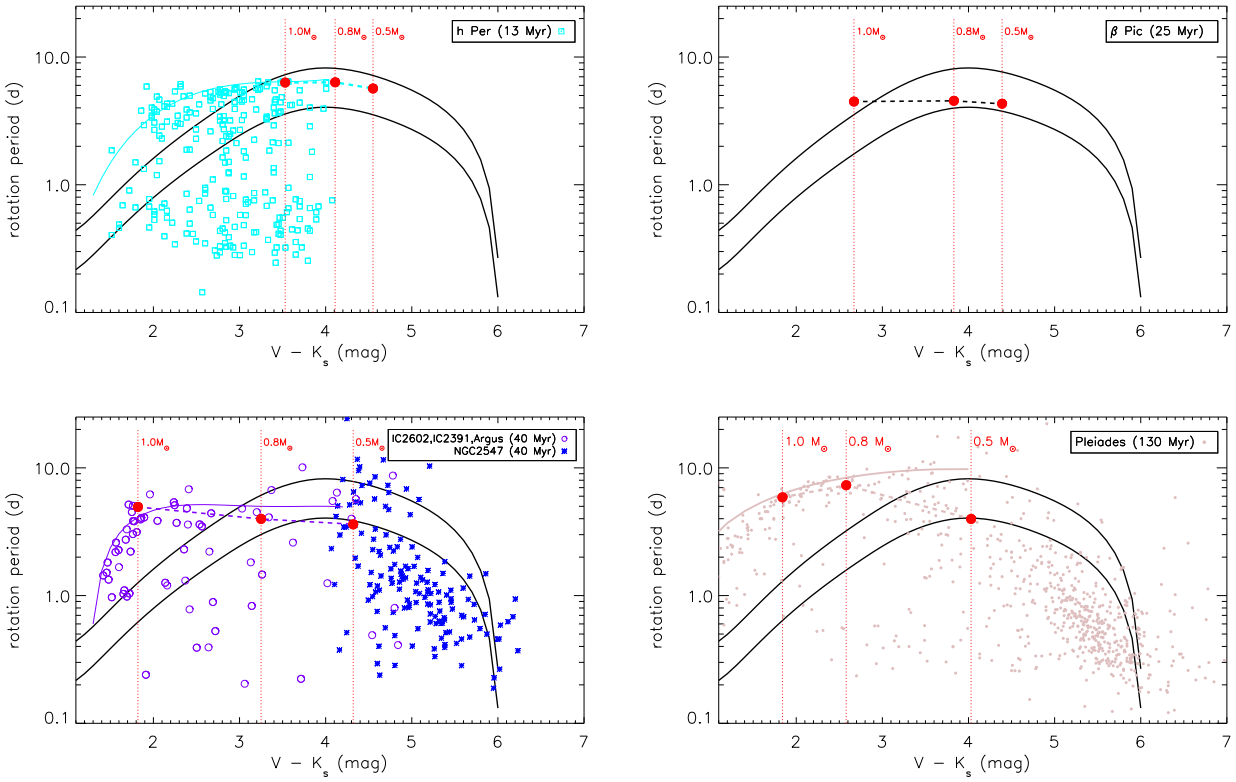

Fig. 8 The rotation period distribution of the β Pic members (only the $\pm 3\sigma$ fits to the distribution are plotted as solid black lines) is compared with the distribution of the h Per single members (light-blue open squares) in the top panel; with the distribution of IC 2391+IC 2602+Argus members (violet open circles), and NGC 2547 members (blue asterisks) in the middle panel, and with the distribution of the Pleiades members (brown small bullets) in the bottom panel. Thick solid lines are linear fits to the 90th percentile of the distribution of the comparison clusters. Filled bullets connected with dashed lines indicate the model rotation period predicted by the Gallet & Bouvier (2015) for 1.0, 0.8 and 0.5 $M_{\odot}$.

age of about 40 Myr have the closest ages to that of β Pictoris and have known rotation period distributions. Unfortunately, we face three major limits when comparing their rotation period distributions. First, the single/binary nature of the comparison cluster and association members is not known as accurately as for the β Pictoris members. For this reason, we will limit the comparison to the upper envelopes of the period distributions, which are likely represented by single stars and wide-orbit binaries. Second, we know the rotation periods of only the higher mass members ($1 < (V-K_s)_0 < 4$ mag) of h Persei. Therefore, at the lower mass regime the comparison is possible only at three time steps (25, 40, and 130 Myr.) Finally, loose and very sparse associations, as β Pictoris, and open clusters may represent two different environments for the dynamical evolution of their members, in the sense that effects of binary encounters on the primordial disc lifetime and, therefore, on the early rotational evolution may be different in magnitude (see, Clarke & Pringle 1993, Heller 1995). Therefore, any results should take into account this major difference.

To compare the distributions, we correct the $V-K_s$ color of the h Per members for interstellar reddening comparing masses and colors taken from Moraux et al. (2013) with the $V-K_s$ versus mass relation for young stars from Pecaut & Mamajek (2013). As a check, we find that the average color excess $E(V-K_s) = 1.60$ mag derived with our approach is in good agreement with the $E(V-K_s) = 1.52$ mag inferred from $E(B-V) = 0.54$ mag (Mayne & Naylor 2008), assuming $R_V = 3.1$. Although we have indication on which members of h Persei are photometric binaries, we do not know the projected separation of their components, therefore we have no possibility to distinguish close from wide orbit binaries, as we did for the β Pictoris members. For this reason, we focus on only the single members of h Persei.

We proceed similarly with the NGC 2547 members using the colors and masses provided by Irwin et al. (2008). However, in this case we infer an average color excess $E(V-K_s) = 0.53$ mag significantly larger than $E(V-K_s) = 0.20$ mag derived from the $E(B-V) = 0.06$ mag (Irwin et al. 2008). The reason of this discrepancy is not clear to us. However, irrespectively from the use of the smaller or larger reddening correction, when we overplot the rotation period distribution of the NGC 2547 members on the rotation period distribution of the β Pictoris bona fide members, we find qualitatively the same result. For the NGC 2547 members we have no indication on their single or binary nature.

The $V-K_s$ colors of the IC 2391, IC 2602, and Argus members were derived using the K_s magnitudes from 2MASS catalog (Cutri et al. 2003) and V magnitudes from Messina et al. (2011) and Barnes et al. (1999).

The results of the comparison are summarized in the

panels of Fig. 8. The comparison period distributions clearly exhibits fast and slow rotators. We use the 90th percentiles computed in 0.5-mag color bins to identify the upper envelope of the rotation period distributions of the comparison cluster and associations. These are represented with heavy solid lines (light-blue for h Persei in the top panel, violet for IC 2391+IC 2602+Argus in the middle panel, and brown for Pleiades in the bottom panel) that mark the position of the slowest members.

The slow F-G members of h Persei and of IC 2391+IC 2602+Argus rotate significantly slower than the F-G members of β Pictoris. Using the known scenario of PMS angular momentum evolution as guideline, we can infer from Fig. 8 that F-G stars at an age of about 13 Myr (h Persei members) are still spinning up, owing to radius contraction and angular momentum conservation. They reach a likely maximum rotation rate at an age of about 25 Myr (β Pictoris members), then after start to slow down, owing to the combined effect of rotation braking by magnetized stellar winds and core-envelope decoupling (see, e.g. Spada et al. 2011), gaining by the age of about 40 Myr the position in the color-period diagram occupied by the IC 2391+IC 2602+Argus slow members. The rotation magnetic braking keeps going with age as shown, for comparison, by the Pleiades members (bottom panel; Rebull et al. 2016) at an age of about 130 Myr. Such an observational pattern is predicted quite well by models of angular momentum evolution for $1.0\,M_{\odot}$ and $0.8\,M_{\odot}$ stars. In Fig. 8 we plot the Gallet & Bouvier (2015) model rotation periods at the sampled ages with filled bullets connected by dashed lines. Vertical dotted lines indicate the $V-K_s$ colors corresponding to $1.0\,M_{\odot}$, $0.8\,M_{\odot}$, and $0.5\,M_{\odot}$ derived from the Baraffe et al. (2008) models used by Gallet & Bouvier (2015). Some level of disagreement exists for $0.8\,M_{\odot}$ stars at 25 Myr and 40 Myr, where model periods are shorter than observed.

Among the slow mid-K to early-M stars it is more complicated to retrieve the angular momentum evolution pattern since these stars have distributions that apparently do not differ significantly from each other at the three time steps 25 Myr, 40 Myr and 130 Myr, giving some hint that the angular momentum evolution of mid-K to early-M stars has been negligible in the 25–130 Myr time interval. The models of angular momentum evolution actually predict a monotonic increase of the rotation rate only from 13 to 40 Myr, and about a constant rotation period up to 130 Myr for the $0.5\,M_{\odot}$ stars (see, e.g. Gallet & Bouvier 2015).

Finally, among the mid- to late-M stars we note that the rotation period distributions at the 40 Myr and 130 Myr steps are about indistinguishable and their upper envelope, consisting of the slow rotators, is below the distribution of the β Pictoris members. We can interpret this result assuming that mid- to late-M stars undergo the stellar radius contraction until about the age of the Pleiades and, therefore, they are observed to spinning up their rotation period from the age of β Pictoris until the Pleiades age, when models of angular momentum evolution predict these stars to reach the maximum rotation rate.

The result that we found for the F and G stars is very important and should be kept in mind when using the rotation period as age indicator. In fact, we found that in the age range from ∼13 Myr to ∼40 Myr the dependence of the rotation period of either single stars or wide components of multiple systems on age is ambiguous. Stars with ages in the 13–25 Myr range (when periods are spinning up) are expected to have again a similar period in the 25–40 Myr range (when periods are slowing down). The uncertainty on the age determination of F–G stars will be minimum at 25 Myr and progressively larger as far as we move to younger or older (up to 40 Myr) ages. On the other hand, such a kind of degeneracy in the age estimate can be successfully removed when the complementary information on the Li EW is available.

7. Light curve amplitude versus rotation

The photometric rotational modulation exhibited by all targets arises from the presence of spots unevenly distributed along their stellar longitudes. The peak-to-peak amplitude of this modulation depends on the spot's area, its temperature contrast with respect to the unspotted photosphere, the photometric band, and on a combination of average latitude where spots are located and the inclination of the stellar rotation axis with respect to the observer's line of sight. These last quantities can play in reducing the observed amplitude for a fixed spot area and temperature contrast.

Moreover, the light curve amplitude generally changes versus time on the same star due to active region growth and decay, latitude migration, and presence of spot cycles and/or long-term trends.

This is the reason why stars of similar masses, rotation periods, and ages show a distribution of amplitudes. The amplitude can be then used as an indicator of a lower limit to the level of activity hosted by the star and, when a series of amplitude measurements are available for a given star, the largest value better represents the maximum activity level that the star can exhibit (see, e.g., Messina et al. 2001, 2003).

The correlation between light curve amplitude and rotation period was earlier investigated in β Pictoris members by Messina et al. (2010, 2011) who found no significant correlation. However, the number of available amplitude measurements for each association was not large as in the present case of the β Pictoris association. Moreover, in those studies no distinction was made between single/wide components of multiple systems and components of close binaries.

In Fig. 9, the light curve amplitudes of the β Pictoris members are plotted versus $\sin i$. Light curve amplitudes, stellar radii, rotation periods, and projected rotational velocities used to derive $\sin i$ are all taken from Paper II. We find that the candidate members (plotted with asterisks) that are single or components of wide binaries, and that were found in our previous analysis to have rotation periods that well fit into the period distribution of bona fide members, have a distribution of amplitudes indistinguishable from that of bona fide members. These stars will be also considered in the following analysis. Light curve amplitudes are measured from the amplitude of the sinusoidal fit to the phased light curves. We find with a Kolmogorov test that single stars and wide components of binary/triple systems exhibit the same distribution. This circumstance further confirms that wide components of multiple systems behave as single stars also on the photometric variability point of view.

From the top panel of Fig. 9, we infer that the amplitude is positively correlated to the $\sin i$ with a Spearman rank cor-

relation $\rho = 0.53$ and p-value 10^{-3}. This result is expected since equator-on stars ($\sin i = 1$) maximize the amplitude of the rotational modulation of starspots with respect to low-inclination ($\sin i < 1$) stars.
We can use the linear fit (solid line) to remove the effect of inclination on the amplitude distribution and compute new amplitudes as all stars were equator-on. Then, in the middle panel of Fig. 9, we plot these inclination-corrected amplitudes versus rotation period. We find a Spearman rank correlation $\rho = 0.06$ and p-value ~ 0.50 that allows us to conclude that the amplitude is not correlated to the rotation. This is a very different behavior with respect to older stars, like the AB Doradus and the Pleiades members (see, Messina et al. 2001, 2003) whose light curve amplitudes are strongly and negatively correlated to the rotation period. We still note a significant dispersion of the amplitudes around their mean value.
In the bottom panel of Fig. 9, we investigate the dependence of the light curve amplitude on the color, i.e. on the stellar mass. Again we find no correlation with a Spearman rank correlation $\rho = 0.02$ and p-value $\sim$0.30. Again, the amplitudes show a level of dispersion that we attribute to the variable level of activity with time. We note an increases of dispersion, with the highest values around K and early-M stars.
Similar results are reported by Moraux et al. (2013) for the h Per cluster at the age of 13 Myr. They find the light curve amplitudes to be uncorrelated to the rotation period. Rather, a week dependence on mass is found, with the lower mass stars to have light curve amplitudes slightly larger than higher mass stars. Similarly at the older age of 40 Myr, the light curve amplitudes of the NGC 2547 members still appear to be uncorrelated to the rotation period (Irwin et al. 2008). Three single stars TYC 915 1391 1 (with no $v \sin i$), TYC 9073 0762 1, and 2MASS J21100535-1919573 all have amplitudes significantly larger than the average (>0.29 mag). These certainly deserve additional study.

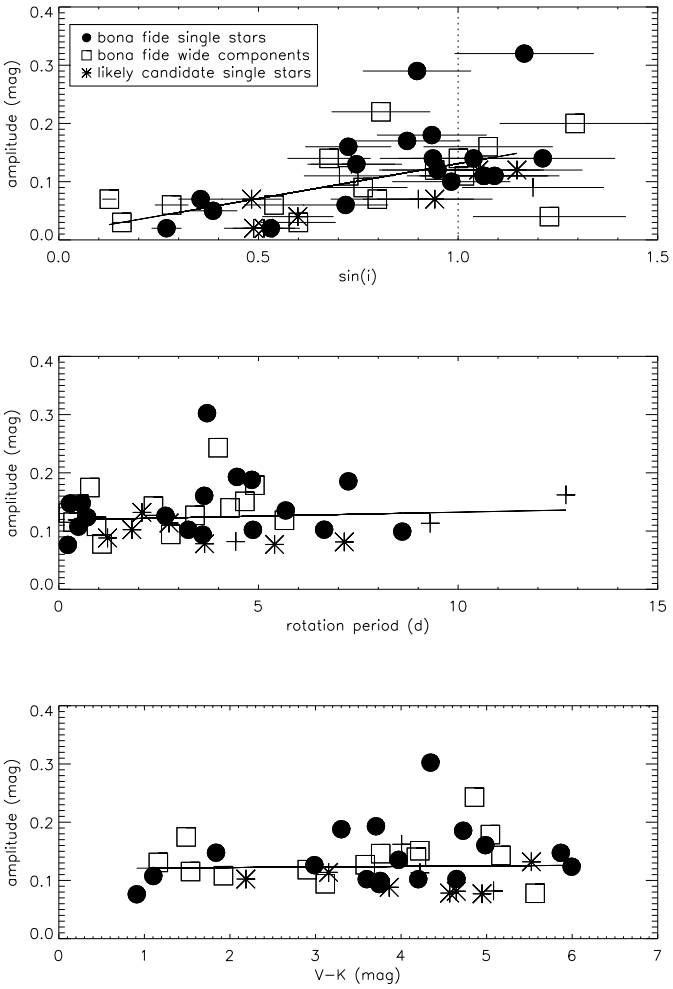

Fig. 9 Top panel: Distribution of V-band light curve amplitudes versus $\sin i$ for bona fide members that are single stars (bullets), wide components of multiple systems (open squares), and single likely candidate members. Middle panel: same as in the top panel but with amplitudes decorrelated from $\sin i$. Bottom panel: Distribution of decorrelated amplitude versus $V-K_s$ color. Solid lines in all panels represent linear fits.

8. Conclusions

We have assessed the membership of the β Pictoris association members using Galactic velocity (UVW) and space (XYZ) components derived from updated values of proper motions, radial velocities, and distances, complemented with information on Li content, and rotation period. As result, we have identified 80 bona fide members, 22 candidate members, and 15 non members on a total of 117 stars.

Analyzing the sample of bona fide members, we found that single stars and components of multiple systems with separation larger than about 80 AU have the same distribution of rotation periods vs. the $V-K_s$ color. On the contrary, components of close visual binaries/triples with separation smaller than about 80 AU rotate preferentially faster than their equal-mass single counterparts. This circumstance suggests that when the components are sufficiently close, their primordial discs undergo an enhanced dispersal allowing the stars to start their spin up earlier that single stars.
The characterization of the period distribution made by us and based on bona fide members, has allowed us to infer additional information on candidate members whose single/binary nature is known. As result of this comparison, we find that among our candidate members 17 stars (five single stars, six wide orbit components, and eight close orbit components of multiple system) have rotation periods that further support their membership. On the contrary, three candidate members (one single star and two close components of multiple systems) have rotation periods that favor their non membership.
All but one spectroscopic binaries in our sample have rotation periods that are not immediately comparable with those of either single/wide components or close components of multiple systems since they likely suffered significantly from tidal effects.
A comparison with the rotation period distributions of the younger h Persei open cluster ($\sim$13 Myr) and the older 40-

Myr IC 2391, IC 2602, Argus, NGC 2547 and the 130-Myr Pleiades members shows that F and G stars at the age of 13 Myr have not reached yet the zero-age-main-sequence and, therefore, are still contracting their radius spinning up their rotation. They reach a likely maximum rotation rate at the age of about 25 Myr (represented by the β Pictoris members). Subsequently, they start a monotonic rotation slowing down which, in our comparison, is readily visible until the Pleiades age. This is the scenario also predicted by models of angular momentum evolution. Differently than model prediction, the K and early-M stars in our sample exhibit period distributions that are apparently indistinguishable from each other. That means that in this mass range the single and wide components β Pictoris members apparently have rotation periods similar to those of either younger or older stars. However, this mass range in our comparison is not represented as significantly as the F and G mass range. Finally, mid- to late-M stars older than 25 Myr all appear to rotate significantly faster than the β Pictoris members, giving hint that the rotation spinning up is proceeding in this mass range. Finally, we find that the distribution of light curve amplitudes of single stars is undistinguishable from that of wide components of multiple systems. Moreover, the amplitude is found to increase with $\sin i$, as expected from geometrical considerations. After decorrelating the dependence on $\sin i$, we found no dependence of the amplitude on the rotation period.

Acknowledgements. Research on stellar activity at INAF- Catania Astrophysical Observatory is supported by MIUR (Ministero dell'Istruzione, dell'Università e della Ricerca). This research has made use of the Simbad database, operated at CDS (Strasbourg, France). LZ acknowledges support by the Joint Research Fund in Astronomy (U1431114 and U1631236) under cooperative agreement between the National Natural Science Foundation of China and Chinese Academy of Sciences. We are very grateful to the Referee whose valuable comments helped us to significantly improve the quality of the paper.

References

Alexander, R. 2012, ApJ, 757, L29
Artymowicz, P. 1992, PASP, 104, 769
Baraffe, I., Chabrier, G., & Barman, T. 2008, A&A, 482, 315
Barnes, S. A., Sofia, S., Prosser, C. F., & Stauffer, J. R. 1999, ApJ, 516, 263
Barrado y Navascués, D., Stauffer, J. R., Song, I., & Caillault, J.-P. 1999, ApJ, 520, L123
Berta, Z. K., Irwin, J., Charbonneau, D., Burke, C. J., & Falco, E. E. 2012, AJ, 144, 145
Beuzit, J.-L., Feldt, M., Dohlen, K., et al. 2008, in Proc. SPIE, Vol. 7014, Ground-based and Airborne Instrumentation for Astronomy II, 701418
Biller, B. A., Liu, M. C., Wahhaj, Z., et al. 2013, ApJ, 777, 160
Bouvier, J., Cabrit, S., Fernandez, M., Martin, E. L., & Matthews, J. M. 1993, A&A, 272, 176
Bouvier, J., Lanzafame, A. C., Venuti, L., et al. 2016, A&A, 590, A78
Brandt, T. D., Kuzuhara, M., McElwain, M. W., et al. 2014, ApJ, 786, 1
Butters, O. W., West, R. G., Anderson, D. R., et al. 2010, A&A, 520, L10
Chauvin, G., Lagrange, A.-M., Beust, H., et al. 2012, A&A, 542, A41
Cieza, L. A., Padgett, D. L., Allen, L. E., et al. 2009, ApJ, 696, L84
Clarke, C. J. & Pringle, J. E. 1993, MNRAS, 261, 190
Cutispoto, G., Messina, S., & Rodonò, M. 2003, A&A, 400, 659
Cutri, R. M., Skrutskie, M. F., van Dyk, S., et al. 2003, 2MASS All Sky Catalog of point sources.
da Silva, L., Torres, C. A. O., de La Reza, R., et al. 2009, A&A, 508, 833
Desidera, S., Covino, E., Messina, S., et al. 2015, A&A, 573, A126
Domingo, A., Gutiérrez-Sánchez, R., Rísquez, D., et al. 2010, Astrophysics and Space Science Proceedings, 14, 493
Douglas, S. T., Agüeros, M. A., Covey, K. R., et al. 2016, ApJ, 822, 47
Drake, A. J., Djorgovski, S. G., Mahabal, A., et al. 2009, ApJ, 696, 870
Edwards, S., Strom, S. E., Hartigan, P., et al. 1993, AJ, 106, 372
Elliott, P., Bayo, A., Melo, C. H. F., et al. 2014, A&A, 568, A26
Gallet, F. & Bouvier, J. 2013, A&A, 556, A36
Gallet, F. & Bouvier, J. 2015, A&A, 577, A98
Heller, C. H. 1995, ApJ, 455, 252
Ingleby, L., Calvet, N., Hernández, J., et al. 2014, ApJ, 790, 47
Irwin, J., Hodgkin, S., Aigrain, S., et al. 2008, MNRAS, 383, 1588
Kiss, L. L., Moór, A., Szalai, T., et al. 2011, MNRAS, 411, 117
Kraus, A. L., Ireland, M. J., Huber, D., Mann, A. W., & Dupuy, T. J. 2016, AJ, 152, 8
Lépine, S. & Simon, M. 2009, AJ, 137, 3632
Malo, L., Artigau, É., Doyon, R., et al. 2014a, ApJ, 788, 81
Malo, L., Doyon, R., Feiden, G. A., et al. 2014b, ApJ, 792, 37
Malo, L., Doyon, R., Lafrenière, D., et al. 2013, ApJ, 762, 88
Mayne, N. J. & Naylor, T. 2008, MNRAS, 386, 261
Meibom, S., Mathieu, R. D., & Stassun, K. G. 2007, ApJ, 665, L155
Messina, S., Desidera, S., Lanzafame, A. C., Turatto, M., & Guinan, E. F. 2011, A&A, 532, A10
Messina, S., Desidera, S., Turatto, M., Lanzafame, A. C., & Guinan, E. F. 2010, A&A, 520, A15
Messina, S., Hentunen, V.-P., & Zambelli, R. 2015a, Information Bulletin on Variable Stars, 6145
Messina, S., Lanzafame, A. C., Feiden, G. A., et al. 2016a, A&A, 596, A29 (Paper I)
Messina, S., Millward, M., Buccino, A., et al. 2016b, ArXiv e-prints: 1612.04591 (Paper II)
Messina, S., Monard, B., Biazzo, K., Melo, C. H. F., & Frasca, A. 2014, A&A, 570, A19
Messina, S., Muro Serrano, M., Artemenko, S., et al. 2015b, Ap&SS, 360, 17
Messina, S., Naves, R., & Medhi, B. J. 2016c, New A, 48, 5
Messina, S., Pizzolato, N., Guinan, E. F., & Rodonò, M. 2003, A&A, 410, 671
Messina, S., Rodonò, M., & Guinan, E. F. 2001, A&A, 366, 215
Moraux, E., Artemenko, S., Bouvier, J., et al. 2013, A&A, 560, A13
Olczak, C., Pfalzner, S., & Eckart, A. 2010, A&A, 509, A63
Pallavicini, R., Cutispoto, G., Randich, S., & Gratton, R. 1993, A&A, 267, 145
Papaloizou, J. C. B. & Terquem, C. 1995, MNRAS, 274, 987
Pecaut, M. J. & Mamajek, E. E. 2013, ApJS, 208, 9
Pojmanski, G. 1997, Acta Astron., 47, 467
Rebull, L. M., Stauffer, J. R., Bouvier, J., et al. 2016, AJ, 152, 113
Rebull, L. M., Wolff, S. C., & Strom, S. E. 2004, AJ, 127, 1029
Riedel, A. R., Finch, C. T., Henry, T. J., et al. 2014, AJ, 147, 85
Schlieder, J. E., Lépine, S., & Simon, M. 2010, AJ, 140, 119
Schlieder, J. E., Lépine, S., & Simon, M. 2012, AJ, 143, 80
Shkolnik, E. L., Anglada-Escudé, G., Liu, M. C., et al. 2012, ApJ, 758, 56
Shu, F. H., Najita, J. R., Shang, H., & Li, Z.-Y. 2000, Protostars and Planets IV, 789
Song, I., Zuckerman, B., & Bessell, M. S. 2003, ApJ, 599, 342
Spada, F., Lanzafame, A. C., Lanza, A. F., Messina, S., & Collier Cameron, A. 2011, MNRAS, 416, 447
Stauffer, J., Rebull, L., Bouvier, J., et al. 2016, AJ, 152, 115
Throop, H. B. & Bally, J. 2008, AJ, 135, 2380
Torres, C. A. O., Quast, G. R., da Silva, L., et al. 2006, A&A, 460, 695
Torres, C. A. O., Quast, G. R., Melo, C. H. F., & Sterzik, M. F. 2008, Young Nearby Loose Associations
Witte, M. G. & Savonije, G. J. 2002, A&A, 386, 222
Woźniak, P. R., Vestrand, W. T., Akerlof, C. W., et al. 2004, AJ, 127, 2436
Zahn, J.-P. 1977, A&A, 57, 383
Zuckerman, B., Song, I., Bessell, M. S., & Webb, R. A. 2001, ApJ, 562, L87

Table 1. List of β Pictoris members analysed in this study: name, RA and DEC coordinates, V mag, V−K_s color, spectral type, rotation period and its uncertainty, light curve amplitude, and info on binarity.

Target	RA (J2000)	DEC (J2000)	V (mag)	V−K (mag)	Sp.T	P (d)	ΔP (d)	ΔV (mag)	type
HIP 560	00 06 50.08	-23 06 27.20	6.15	0.91	F3V	0.224	0.005	0.008	S+D
2MASS J00172353-6645124	00 17 23.54	-66 45 12.50	12.35	4.65	M2.5V	6.644	0.027	0.100	S
TYC 1186 0706 1	00 23 34.66	20 14 28.75	10.96	3.62	K7.5V+M5	7.9	0.1	0.070	Bw
GJ 2006A	00 27 50.23	-32 33 06.42	12.87	4.86	M3.5Ve	3.99	0.05	0.170	Bw
GJ 2006B	00 27 50.35	-32 33 23.86	13.16	5.04	M3.5Ve	4.91	0.05	0.120	Bw
2MASS J00323480+0729271A	00 32 34.81	07 29 27.10	13.40	5.02	M4V	3.355	0.005	0.045	Bc
2MASS J00323480+0729271B	00 32 34.81	07 29 27.10	12.62	5.68	>M5	0.925	0.008	0.045	Bc
TYC 5853 1318 1	01 07 11.94	-19 35 36.00	11.41	4.16	M1V	7.26	0.07	0.10	S?
2MASS J01112542+1526214A	01 11 25.42	15 26 21.50	14.46	6.25	M5V	0.911	0.001	0.01	Bc
2MASS J01112542+1526214B	01 11 25.42	15 26 21.50	14.46	6.55	M6V	0.791	0.001	0.01	Bc
2MASS J01132817-3821024	01 13 28.17	-38 21 02.50	11.77	4.17	(M0V+M3V)+M1V	0.446	—	0.210	Tc
2MASS J01351393-0712517	01 35 13.93	-07 12 51.77	13.42	5.50	M4.5V	0.703	—	0.080	SB2
2MASS J01365516-0647379	01 36 55.16	-06 47 37.92	14.00	5.14	M4V+L0	0.346	0.001	0.11	Bw
TYC 1208 0468 1	01 37 39.42	18 35 32.91	9.83	3.11	K3V+K5V	2.803	0.010	0.07	Bw
2MASS J01535076-1459503	01 53 50.77	-14 59 50.30	11.97	4.90	M3V+M3V	1.515	—	0.110	BC
2MASS J02014677+0117161	02 01 46.78	01 17 16.20	12.78	4.51	M	—	—	—	—
RBS 269	02 01 46.93	01 17 06.00	12.72	4.46	M	5.98/3.30	0.01	0.09	Bw
2MASS J02175601+1225266	02 17 56.01	12 25 26.70	13.62	4.54	M3.5V	1.995	0.005	0.05	S
HIP 10679	02 17 24.74	28 44 30.43	7.75	1.49	G2V	0.777	0.005	0.070	Bw+D
HIP 10680	02 17 25.28	28 44 42.16	6.95	1.16	F5V	0.240	0.001	0.030	Bw
HIP 11152	02 23 26.64	+22 44 06.75	11.09	3.74	M3V	1.80/3.60	0.02	0.06	S
HIP 11437A	02 27 29.25	30 58 24.60	10.12	3.04	K4V	12.5	0.5	0.20	Bw+D
HIP 11437B	02 27 28.05	30 58 40.53	12.44	4.22	M1V	4.66	0.05	0.16	Bw
HIP 12545	02 41 25.90	05 59 18.00	10.37	3.30	K6Ve	4.83	0.03	0.180	S
2MASS J03350208+2342356	03 35 02.09	23 42 35.61	17.00	5.74	M8.5V	0.472	0.005	0.03	Bc?
2MASS J03461399+1709176	03 46 14.00	17 09 17.45	12.90	4.08	M0.5	1.742	0.001	0.07	S
GJ 3305	04 37 37.30	-02 29 28.00	10.59	4.18	M1+M?	4.89	0.01	0.05	Bc
2MASS J04435686+3723033	04 43 56.87	37 23 03.30	12.98	4.18	M3Ve+M5?	4.288	—	—	Bw
HIP 23200	04 59 34.83	01 47 00.68	10.05	3.99	M0.5Ve	4.430	0.030	0.150	SB1
TYC 1281 1672 1	05 00 49.28	15 27 00.71	10.75	3.15	K2IV	2.76	0.01	0.12	S
HIP 23309	05 00 47.10	-57 15 25.00	10.00	3.76	M0Ve	8.60	0.07	0.110	S
2MASS J05015665+0108429	05 01 56.65	01 08 42.91	13.20	5.52	M4V	2.08	0.02	0.07	S?
HIP 23418A	05 01 58.80	09 59 00.00	11.45	4.78	M3V	1.220	0.010	0.070	SB2
HIP 23418B	05 01 58.80	09 59 00.00	12.45	5.23	>M3V	—	—	—	Tc
BD -21 1074A	05 06 49.90	-21 35 09.00	10.29	4.35	M1.5V	9.3	0.1	0.120	Tw
BD -21 1074B	05 06 49.90	-21 35 09.00	11.67	4.64	M2.5V	5.40	0.10	0.080	Tc
2MASS J05082729-2101444	05 08 27.30	-21 01 44.40	14.70	5.87	M5.6V	0.280	0.002	0.07	S
TYC 1121 486 1	05 20 31.83	+06 16 11.48	11.67	3.11	K4V	2.18	—	0.09	Tc
TYC 112 917 1	05 20 00.29	+06 13 03.57	11.58	3.00	K4V	3.51	—	0.08	Tw
2MASS J05241914-1601153	05 24 19.15	-16 01 15.30	14.32	5.60	M4.5+M5	0.401	0.001	0.15	Bc
HIP 25486	05 27 04.76	-11 54 03.47	6.22	1.29	F7V	0.966	0.002	0.10	SB2
2MASS J05294468-3239141	05 29 44.68	-32 39 14.20	13.79	5.47	M4.5V	1.532	0.005	0.03	S?
TYC 4770 0797 1	05 32 04.51	-03 05 29.38	11.32	4.31	M2V+M3.5V	4.372	0.002	0.160	Bc
2MASS J05335981-0221325	05 33 59.81	-02 21 32.50	12.42	4.72	M2.9V	7.250	—	0.170	S
2MASS J06131330-2742054	06 13 13.31	-27 42 05.50	12.09	5.23	M3.V:	16.8	1.0	0.07	Tc
HIP 29964	06 18 28.20	-72 02 41.00	9.80	2.99	K4Ve	2.670	0.010	0.120	S+D
2MASS J07293108+3556003AB	07 29 31.09	35 56 00.40	11.82	4.02	M1+M3	1.970	0.010	0.10	Bc
2MASS J08173943-8243298	08 17 39.44	-82 43 29.80	11.62	5.03	M3.5V	1.318	—	0.050	Bc?
2MASS J08224744-5726530	08 22 47.45	-57 26 53.00	13.37	5.57	M4.5+L0	—	—	—	Tc
2MASS J09361593+3731456AB	09 36 15.91	37 31 45.50	11.09	4.10	M0.5+M0.5	12.9	0.3	0.030	SB2
2MASS J10015995+6651278	10 02 00.10	66 51 26.00	12.38	4.16	M3	2.49	0.02	0.060	Bc?
HIP 50156	10 14 19.17	21 04 29.55	10.08	3.82	M0.5V+?	7.860	—	0.050	Bc

Table 1 (cont'd)

Target	RA (J2000)	DEC (J2000)	V (mag)	V−K (mag)	Sp.T	P (d)	ΔP (d)	ΔV (mag)	type
TWA 22	10 17 26.89	-53 54 26.50	13.99	6.30	M5+M6	0.830	0.010	0.020	Bc
BD +26 2161A	10 59 38.31	25 26 15.50	8.45	2.61	K2	2.022/0.974	0.005	0.010	Bw+D
BD +26 2161B	10 59 38.31	25 26 15.50	9.09	3.25	K5	0.974/2.022	0.005	0.010	Bw
2MASS J11515681+0731262	11 51 56.81	07 31 26.25	12.38	4.61	M2+M2+M8	2.291	—	0.130	SB2
2MASS J13545390-7121476	13 54 53.90	-71 21 47.67	12.24	4.57	M2.5V	3.65	0.02	0.020	S?
HIP 69562A	14 14 21.36	-15 21 21.75	10.27	3.67	K5.5V+	0.298	0.005	0.17	Tc
HIP 69562B	14 14 21.36	-15 21 21.75	10.27	3.67	—	—	—	—	Tc
TYC 915 1391 1	14 25 55.93	14 12 10.14	10.89	3.60	K4V	4.340	—	0.360	S
HIP 76629	15 38 57.50	-57 42 27.00	7.97	2.12	K0V	4.27	0.10	0.180	SB1
2MASS J16430128-1754274	16 43 01.29	-17 54 27.50	12.50	3.95	M0.6	5.14	0.04	0.140	S
2MASS J16572029-5343316	16 57 20.30	-53 43 31.70	12.44	4.65	M3V	7.15	0.05	0.020	S
2MASS J17150219-3333398	17 15 02.20	-33 33 39.80	10.93	3.86	M0V	0.311	—	0.110	Bc?
HIP 84586	17 17 25.50	-66 57 04.00	7.23	2.53	G5IV+K5IV	1.680	0.010	0.120	SB2
HD 155555C	17 17 31.29	-66 57 05.49	12.71	5.08	M3.5Ve	4.43	0.01	0.070	Tw
TYC 8728 2262 1	17 29 55.10	-54 15 49.00	9.55	2.19	K1V	1.775	0.005	0.150	S
GSC 08350-01924	17 29 20.67	-50 14 53.00	13.47	4.77	M3V	1.906	0.005	0.05	Bc
HD 160305	17 41 49.03	-50 43 28.00	8.35	1.36	F9V	1.336	0.008	0.060	S+D
TYC 8742 2065 1	17 48 33.70	-53 06 43.00	8.94	2.16	K0IV+	2.60/1.62	0.01	0.060	Tc
HIP 88399	18 03 03.41	-51 38 56.43	12.50	4.23	M2V+F6V	—	—	—	Bw
V4046 Sgr	18 14 10.50	-32 47 33.00	10.44	3.19	K5V+K7V	2.42	0.01	0.090	SB2+D
UCAC2 18035440	18 14 22.07	-32 46 10.12	12.78	4.24	M1Ve	12.05	0.5	0.14	SB
2MASS J18151564-4927472	18 15 15.64	-49 27 47.20	12.86	4.78	M3V	0.447	0.002	0.130	SB1
HIP 89829	18 19 52.20	-29 16 33.00	8.89	1.84	G1V	0.571	0.001	0.140	S
2MASS J18202275-1011131A	18 20 22.74	-10 11 13.62	10.63	3.35	K5Ve	4.65/5.15	—	0.070	Bw+D
2MASS J18202275-1011131B	18 20 22.74	-10 11 13.62	10.63	4.01	K7Ve	5.15/4.65	—	0.070	Bw
2MASS J18420694-5554254	18 42 06.95	-55 54 25.50	13.53	4.95	M3.5V	5.403	—	0.070	S?
TYC 9077 2489 1	18 45 37.02	-64 51 46.14	9.30	3.20	K8Ve	0.345	0.005	0.160	Tc
TYC 9073 0762 1	18 46 52.60	-62 10 36.00	11.80	3.95	M1Ve	5.37	0.04	0.320	S
HD 173167	18 48 06.36	-62 13 47.02	7.28	1.14	F5V	0.290	0.005	0.220	SB1
TYC 740800541	18 50 44.50	-31 47 47.00	11.20	3.66	K8Ve	1.075	0.005	0.150	EB
HIP 92680	18 53 05.90	-50 10 50.00	8.29	1.92	K8Ve	0.944	0.001	0.110	Bw
TYC 6872 1011 1	18 58 04.20	-29 53 05.00	11.78	3.76	M0Ve	0.503	0.004	0.060	Bw
2MASS J19102820-2319486	19 10 28.21	-23 19 48.60	13.20	4.99	M4V	3.64	0.02	0.13	S
TYC 6878 0195 1	19 11 44.70	-26 04 09.00	10.27	2.90	K4Ve	5.70	0.05	0.090	Bw
2MASS J19233820-4606316	19 23 38.20	-46 06 31.60	11.87	3.60	M0V	3.237	—	0.110	S
2MASS J19243494-3442392	19 24 34.95	-34 42 39.30	14.28	5.50	M4V	0.708	0.001	0.020	Bc?
TYC 7443 1102 1	19 56 04.37	-32 07 37.71	11.80	3.95	M0.0V	11.3	0.2	0.09	Tw
2MASS J19560294-3207186AB	19 56 02.94	-32 07 18.70	13.30	5.12	M4V	1.569	0.003	0.030	Tc
2MASS J20013718-3313139	20 01 37.18	-33 13 14.01	12.25	4.06	M1V	12.7	0.2	0.13	Tw
2MASS J20055640-3216591	20 05 56.41	-32 16 59.15	11.96	4.02	M2V	8.368	0.005	0.130	S
HD 191089	20 09 05.21	-26 13 26.52	7.18	1.10	F5V	0.488	0.005	—	S+D
2MASS J20100002-2801410AB	20 10 00.03	-28 01 41.10	13.62	4.64	M2.5+M3.5	0.470	0.005	0.040	Bc
2MASS J20333759-2556521	20 33 37.59	-25 56 52.20	14.87	5.99	M4.5V	0.710	0.001	0.05	S
HIP 102141A	20 41 51.20	-32 26 07.00	11.09	5.42	M4Ve	1.191	0.005	0.040	Bc
HIP 102141B	20 41 51.10	-32 26 10.00	11.13	5.42	M4Ve	0.781	0.002	0.020	Bc
2MASS J20434114-2433534	20 43 41.14	-24 33 53.19	12.83	4.97	M3.7+M4.1	1.610	0.010	0.03	Bc
HIP 102409	20 45 09.50	-31 20 27.00	8.73	4.20	M1Ve	4.86	0.02	0.10	S+D
HIP 103311	20 55 47.67	-17 06 51.04	7.35	1.54	F8V	0.356	0.004	0.06	Bc
TYC 6349 0200 1	20 56 02.70	-17 10 54.00	10.62	3.54	K6Ve+M2	3.41	0.05	0.120	Bw
2MASS J21100535-1919573	21 10 05.36	-19 19 57.40	11.54	4.34	M2V	3.71	0.02	0.29	S
2MASS J21103147-2710578	21 10 31.48	-27 10 57.80	15.20	5.60	M4.5V	1.867	0.008	0.04	Bw
2MASS J21103096-2710513	21 10 30.96	-27 10 51.30	15.72	5.60	M5V	—	—	—	Bw

Table 1 (cont'd)

Target	RA (J2000)	DEC (J2000)	V (mag)	V−K (mag)	Sp.T	P (d)	ΔP (d)	ΔV (mag)	type
HIP 105441	21 21 24.49	-66 54 57.37	8.77	2.37	K2V	5.50	0.02	0.050	Bw
TYC 9114 1267 1	21 21 28.72	-66 55 06.30	10.59	3.58	K7V	20.5	1.0	0.015	Bw
TYC 9486 927 1	21 25 27.49	-81 38 27.68	11.70	4.36	M1V	0.542	—	0.190	Bc
2MASS J21374019+0137137AB	21 37 40.19	01 37 13.70	13.36	5.48	M5V	0.202	0.001	0.130	Bc
2MASS J21412662+2043107	21 41 26.63	20 43 10.70	13.50	4.89	M3V	0.899	0.001	0.03	Bc?
TYC 2211 1309 1	22 00 41.59	27 15 13.60	11.39	3.67	M0V	1.109	0.001	0.080	Bc
TYC 9340 0437 1	22 42 48.90	-71 42 21.00	10.60	3.71	K7Ve	4.46	0.03	0.16	S
HIP 112312	22 44 58.00	-33 15 02.00	12.10	5.17	M4Ve	2.37	0.01	0.110	Bw
TX Psa	22 45 00.05	-33 15 25.80	13.36	5.57	M4.5Ve	1.080	0.005	0.030	Bw
2MASS J22571130+3639451	22 57 11.31	36 39 45.14	12.50	3.86	M3V	1.220	0.020	0.04	S
TYC 5832 0666 1	23 32 30.90	-12 15 52.00	10.54	3.97	M0Ve	5.68	0.03	0.140	S
2MASS J23500639+2659519	23 50 06.39	26 59 51.93	14.26	4.96	M3.5V	0.287	0.005	0.05	Bc?
2MASS J23512227+2344207	23 51 22.28	23 44 20.80	14.11	5.29	M4V	3.208	0.004	0.060	S

Table 4. Results of membership assessment based on velocity (U, V, W), space (X, Y, Z) components, Li EW, and rotation period (P)

Target	U	V	W	X	Y	Z	Li	P	final	Note
HIP 560	Y	Y	Y	Y	Y	Y	Y	Y	Y	Core
2MASS J00172353-6645124	Y	Y	Y	Y	Y	Y	-	Y	Y	Core
TYC 1186 0706 1	Y	Y	Y	Y	Y	Y	Y	Y	Y	
GJ 2006A	Y	N	Y	Y	Y	Y	Y	Y	Y	Core
GJ 2006B	Y	Y	Y	Y	Y	Y	Y	Y	Y	Core
2MASS J00323480+072927A	Y	Y	Y	Y	Y	Y	-	?	N	
2MASS J00323480+072927B	Y	Y	Y	Y	Y	Y	-	?	N	
TYC 5853 1318 1	N	N	Y	Y	Y	Y	-	Y	Y	C
2MASS J01112542+1526214A	Y	Y	Y	Y	Y	Y	Y	-	Y	
2MASS J01112542+1526214B	Y	Y	Y	Y	Y	Y	-	-	Y	
2MASS J01132817-3821024	Y	Y	Y	Y	Y	Y	-	Y	Y	
2MASS J01351393-0712517	Y	Y	Y	Y	Y	Y	Y	-	Y	
2MASS J01365516-0647379	Y	Y	Y	Y	Y	Y	N	N	N	
TYC 1208 0468 1	Y	Y	Y	Y	Y	Y	Y	N	Y	C
2MASS J01535076-1459503	Y	Y	Y	Y	Y	Y	-	Y	Y	
2MASS J02014677+0117161	Y	N	Y	Y	Y	N	-	Y	Y	Core_e
RBS 269	Y	N	Y	Y	Y	N	-	Y	Y	Core_e
2MASS J02175601+1225266	Y	N	Y	Y	Y	N	-	N	Y	Core_e
HIP 10679	Y	Y	Y	Y	Y	Y	Y	Y	Y	Core
HIP 10680	Y	Y	Y	Y	Y	Y	Y	Y	Y	Core
HIP 11152	Y	Y	Y	Y	Y	Y	-	Y	Y	Core
HIP 11437A	Y	Y	Y	Y	Y	Y	N	N	Y	Core
HIP 11437B	Y	Y	Y	Y	Y	Y	Y	Y	Y	Core
HIP 12545	Y	Y	Y	Y	Y	Y	Y	Y	Y	Core
2MASS J03350208+2342356	Y	N	Y	Y	Y	Y	-	Y	Y	C
2MASS J03461399+1709176	N	N	N	Y	Y	Y	-	N	N	
GJ 3305	N	Y	Y	Y	Y	Y	Y	U	?	C
2MASS J04435686+3723033	Y	N	N	Y	Y	Y	Y	Y	Y	Core_e
HIP 23200	Y	Y	Y	Y	Y	Y	Y	-	Y	
TYC 1281 1672 1	Y	Y	Y	Y	Y	Y	-	Y	Y	
HIP 23309	Y	Y	Y	Y	Y	Y	Y	Y	Y	
2MASS J05015665+0108429	Y	Y	Y	Y	Y	Y	-	Y	Y	
HIP 23418A	Y	Y	Y	Y	Y	Y	Y	-	Y	
HIP 23418B	Y	Y	Y	Y	Y	Y	-	-	Y	
BD -21 1074A	Y	Y	Y	Y	Y	Y	Y	N	Y	Core
BD -21 1074B	Y	Y	N	Y	Y	Y	Y	N	N	C
2MASS J05082729-2101444	Y	Y	Y	Y	Y	Y	Y	Y	Y	Core
TYC 112 1486 1	Y	Y	Y	Y	Y	Y	-	Y	Y	
TYC 112 917 1	Y	Y	Y	Y	Y	Y	-	Y	Y	
2MASS J05241914-1601153	Y	Y	Y	Y	Y	Y	Y	Y	Y	
HIP 25486	Y	Y	Y	Y	Y	Y	Y	-	Y	
2MASS J05294468-3239141	N	N	N	Y	Y	Y	-	Y	Y	C
TYC 4770 0797 1	Y	Y	Y	Y	Y	Y	-	N	N	C
2MASS J05335981-0221325	Y	Y	Y	Y	Y	Y	Y	Y	Y	Core
2MASS J06131330-2742054	Y	Y	Y	Y	Y	Y	Y	N	Y	
HIP 29964	Y	Y	Y	Y	Y	Y	Y	Y	Y	Core
2MASS J07293108+3556003AB	Y	Y	Y	Y	Y	N	-	Y	Y	C
2MASS J08173943-8243298	Y	Y	Y	Y	Y	Y	-	Y	Y	
2MASS J08224744-5726530	Y	Y	Y	Y	Y	Y	-	-	Y	
2MASS J09361593+3731456AB	Y	Y	N	Y	Y	N	-	-	-	C
2MASS J10015995+6651278	Y	N	Y	Y	Y	N	-	Y	Y	C
HIP 50156	Y	N	N	Y	Y	N	-	N	N	C
TWA 22	Y	Y	Y	Y	Y	Y	Y	-	Y	

Table 4 (cont'd)

Target	U	V	W	X	Y	Z	Li	P	final	Note
BD +26 2161A	N	N	N	N	N	N	-	Y	N	
BD +26 2161B	Y	Y	Y	Y	Y	N	-	N	N	C
2MASS J11515681+0731262	Y	Y	N	Y	Y	N	-	-		C
2MASS J13545390-7121476	Y	Y	Y	Y	Y	Y	-	Y	Y	
HIP 69562A	Y	N	N	Y	Y	N	-	Y	Y	C
HIP 69562B	Y	N	Y	Y	Y	N	-	-	Y	C
TYC 915 1391 1	N	N	N	Y	Y	N	Y	Y	N	
HIP 76629	Y	Y	Y	Y	Y	Y	-	-	Y	
2MASS J16430128-1754274	Y	N	N	Y	Y	N	Y	Y	Y	Core_e
2MASS J16572029-5343316	Y	Y	Y	Y	Y	Y	-	Y	Y	C
2MASS J17150219-3333398	Y	Y	Y	Y	Y	Y	-	Y	Y	
HIP 84586	Y	Y	Y	Y	Y	Y	N	-	Y	
HD 155555C	Y	Y	Y	Y	Y	Y	Y	Y	Y	Core
TYC 8728 2262 1	Y	Y	Y	Y	Y	Y	Y	Y	Y	
GSC 08350-01924	Y	Y	Y	Y	Y	Y	Y	Y	Y	
HD 160305	Y	Y	Y	Y	Y	Y	-	N	Y	
TYC 8742 2065 1	Y	Y	Y	Y	Y	Y	-	N	Y	
HIP 88399	Y	Y	Y	Y	Y	Y	-	Y	Y	Core
V4046 Sgr	Y	Y	Y	Y	Y	Y	Y	-	Y	
UCAC2 18035440	N	N	N	N	N	N	-	-	N	
2MASS J18151564-4927472	N	Y	Y	Y	Y	Y	Y	-	-	C
HIP 89829	Y	Y	Y	Y	Y	Y	Y	Y	Y	Core
2MASS J18202275-1011131A	N	Y	Y	Y	Y	N	Y	Y	Y	C
2MASS J18202275-1011131B	N	Y	Y	Y	Y	N	-	Y	Y	C
2MASS J18420694-5554254	Y	Y	Y	Y	Y	Y	-	Y	Y	
TYC907724891	Y	Y	Y	Y	Y	Y	Y	Y	Y	
TYC 9073 0762 1	Y	Y	Y	Y	Y	Y	Y	Y	Y	Core
HD 173167	Y	Y	Y	Y	Y	Y	Y	-	Y	
TYC 7408 0054 1	Y	Y	Y	Y	Y	Y	Y	-	Y	
HIP 92680	Y	Y	Y	Y	Y	Y	Y	Y	Y	Core
TYC 6872 1011 1	N	Y	Y	Y	Y	Y	Y	N	Y	Core_e
2MASS J19102820-2319486	Y	Y	Y	Y	Y	Y	Y	Y	Y	Core
TYC 6878 0195 1	Y	Y	Y	Y	Y	Y	N	N	Y	Core
2MASS J19233820-4606316	Y	Y	Y	Y	Y	Y	Y	Y	Y	Core
2MASS J19243494-3442392	Y	Y	Y	Y	Y	Y	-	Y	Y	
TYC 7443 1102 1	Y	Y	Y	Y	Y	Y	Y	N	Y	Core
2MASS J19560294-3207186AB	Y	Y	Y	Y	Y	Y	Y	Y	Y	
2MASS J20013718-3313139	Y	Y	Y	Y	Y	Y	Y	N	Y	Core
2MASS J20055640-3216591	N	N	N	N	N	N	Y	Y	N	
HD 191089	Y	Y	Y	Y	Y	Y	Y	Y	Y	Core
2MASS J20100002-2801410AB	Y	Y	Y	Y	Y	Y	Y	Y	Y	
2MASS J20333759-2556521	Y	Y	Y	Y	Y	Y	Y	Y	Y	Core
HIP 102141A	Y	Y	Y	Y	Y	Y	Y	Y	Y	
HIP 102141B	Y	Y	Y	Y	Y	Y	Y	Y	Y	
2MASS J20434114-2433534	Y	N	N	Y	Y	Y	Y	Y	Y	C
HIP 102409	Y	Y	Y	Y	Y	Y	Y	Y	Y	Core
HIP 103311	N	Y	N	Y	Y	Y	Y	Y	Y	C
TYC 6349 0200 1	Y	Y	Y	Y	Y	Y	Y	Y	Y	Core
2MASS J21100535-1919573	Y	Y	Y	Y	Y	Y	Y	Y	Y	Core
2MASS J21103147-2710578	Y	Y	Y	Y	Y	Y	Y	Y	Y	Core
2MASS J21103096-2710513	Y	Y	Y	Y	Y	Y	-	Y	Y	Core
HIP 105441	Y	Y	Y	Y	Y	Y	N	N	N	
TYC 9114 1267 1	Y	Y	Y	Y	Y	Y	N	N	N	

Table 4 (cont'd)

Target	U	V	W	X	Y	Z	Li	P	final	Note
TYC 9486 927 1	N	Y	Y	Y	Y	Y	Y	Y	Y	C
2MASS J21374019+0137137AB	Y	N	N	Y	Y	Y	-	Y	Y	C
2MASS J21412662+2043107	Y	Y	Y	Y	N	Y	-	Y	Y	C
TYC 2211 1309 1	Y	N	Y	Y	Y	Y	Y	-	-	C
TYC 9340 0437 1	Y	Y	Y	Y	Y	Y	Y	Y	Y	Core
HIP 112312	Y	Y	Y	Y	Y	Y	Y	Y	Y	Core
TX Psa	Y	Y	Y	Y	Y	Y	Y	N	Y	Core
2MASS J22571130+3639451	Y	N	N	Y	N	Y	-	N	N	
TYC 5832 0666 1	Y	Y	Y	Y	Y	Y	Y	Y	Y	Core
2MASS J23500639+2659519	Y	Y	Y	Y	Y	Y	-	Y	Y	
2MASS J23512227+2344207	Y	Y	Y	Y	Y	Y	-	Y	Y	C

Core: core member; Core_e: core member excluded from fit; C: candidate